NASA CR–66692
BRL NO. 4455

Research and Development of a Vortex Valve Controlled Hot Gas (5500°F) Secondary Injection Thrust Vector Control System

By
T.W. Keranen and A. Blatter

September 1968

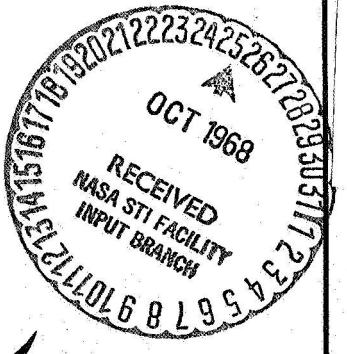

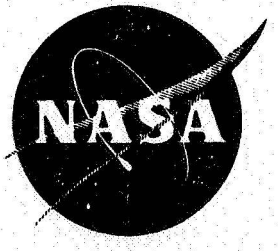

Prepared Under Contract No. NAS 1–5199

NATIONAL AERONAUTICS AND SPACE ADMINISTRATION

Bendix
Research
Laboratories

NASA CR–66692
BRL NO. 4455

Research and Development of a Vortex Valve Controlled Hot Gas [5500°F] Secondary Injection Thrust Vector Control System

By
T.W. Keranen and A. Blatter

Prepared under Contract No. NAS 1–5199 by
BENDIX RESEARCH LABORATORIES
Southfield, Michigan 48075

for
NATIONAL AERONAUTICS AND SPACE ADMINISTRATION

Research Laboratories

TABLE OF CONTENTS

	Page
SUMMARY	1
INTRODUCTION	2
Secondary Injection Thrust Vector Control Concept	2
Program Description	2
SITVC SYSTEM DESCRIPTION	5
System Operation	5
System Design	7
Rocket Motor and Test Stand Description	11
TEST RESULTS	12
Cold Gas Test Results	12
Hot Gas Test Results	12
Test Conclusions	39
CONCLUSIONS AND RECOMMENDATIONS	40
Conclusions	40
Recommendations	40
APPENDIX - SITVC PERFORMANCE ANALYSIS	42
GLOSSARY OF SYMBOLS	49
REFERENCES	50
BIBLIOGRAPHY	50
ABSTRACT	51

LIST OF ILLUSTRATIONS

Figure No.	Title	Page
1	Conceptual Vortex Valve Secondary Injection Thrust Vector Control System - Buried Nozzle Installation	3
2	Schematic of Vortex Valve Controlled SITVC System	6
3	5500°F Vortex Valve	6
4	Vortex Valve Installation on the EM-72 Rocket Motor Nozzle	8
5	5500°F Vortex Valve Configuration, Basic Dimensions and Materials	9
6	Main Stage Vortex Valve Weeping Orifice Flow Measurement System	9
7	Disassembled View of the 5500°F SITVC System Pilot Stage	10
8	Thrust Stand Transducer Locations	11
9	Main Stage SITVC Vortex Valve No. 1 - Cold Gas Turndown Performance	13
10	Main Stage SITVC Vortex Valve No. 2 - Cold Gas Turndown Performance	13
11	Pressure Tap and Weeping Orifice Cold Gas Flow Calibration (Corrected to Hot Gas Flow)	14
12	Test Schematic for Cold Gas Test for the SITVC System	14
13	SITVC System Cold Gas Test Performance	15
14	Schematic of Hot Gas Test System	16
15	Vortex Valve Controlled SITVC System Installation on EM-72 Rocket Motor - Component Location	17
16	Vortex Valve Controlled SITVC System Installation on EM-72 Rocket Motor - Side View	17
17	Vortex Valve Controlled SITVC System Installation on EM-72 Rocket Motor - Side View	18
18	Vortex Valve SITVC System Duty Cycle for EM-72 Rocket Motor and Bendix Controls	18
19	EM-72 Rocket Motor Operating Pressure	20
20	EM-72 Rocket Motor Axial Thrust	20
21	2000°F SPGG Operating Pressure	21
22	5500°F SPGG Operating Pressure	21
23	SITVC System Pressure Distribution - Test Time 4.3 Second	22
24	SITVC System Pressure Distribution - Test Time 12 Second	22
25	SITVC System Pressure Distribution - Test Time 24 Second	23
26	SITVC System Pressure Distribution - Test Time 28 Second	23
27	SITVC Vortex Valve Weeping Orifice Flow Measurements Pressures P45 and P46	25

Figure No.	Title	Page
28	Pilot Stage Pressures P35 and P37	25
29	EM-72 Rocket Motor Yaw and Pitch Forces - Command Input 2 Hertz	26
30	EM-72 Rocket Motor Yaw and Pitch Forces - Command Input 4 Hertz	26
31	EM-72 Rocket Motor Yaw and Pitch Forces - Command Input 8 Hertz	27
32	EM-72 Rocket Motor Yaw and Pitch Forces - Command Input 16 Hertz	27
33	Effectiveness of Hot Gas Injection Compared to Cold Gas and Liquid Injectants	29
34	Amplitude Versus Frequency, Yaw Plane of Vortex Valve Controlled SITVC System on EM-72 Rocket Engine	31
35	Phase Angle Versus Frequency, Yaw Plane of Vortex Valve Controlled SITVC System on EM-72 Rocket Engine	31
36	Amplitude Versus Frequency, Pitch Plane of Vortex Controlled SITVC System on EM-72 Rocket Engine	32
37	Phase Angle Versus Frequency, Pitch Plane of Vortex Valve Controlled SITVC System on EM-72 Rocket Engine	32
38(a)	Nozzle Pressure Probe Map - Time 4.155	33
38(b)	Nozzle Pressure Probe Map - Time 4.187	33
38(c)	Nozzle Pressure Probe Map - Time 4.220	34
38(d)	Nozzle Pressure Probe Map - Time 4.255	34
38(e)	Nozzle Pressure Probe Map - Time 4.285	35
38(f)	Nozzle Pressure Probe Map - Time 4.318	35
38(g)	Nozzle Pressure Probe Map - Time 4.351	36
38(h)	Nozzle Pressure Probe Map - Time 4.387	36
38(i)	Nozzle Pressure Probe Map - Time 4.420	37
38(j)	Nozzle Pressure Probe Map - Time 4.452	37
38(k)	Nozzle Pressure Probe Map - Time 4.485	38
39	Post Test, Interior of Hot Gas SITVC Vortex Valve	38
40	System Parameters and Variables	45
41	Shock Angle, Separation Angle and Pressure Ratios Versus Primary Mach Number at Shock Apex	46
42	Area Ratio, Pressure Ratio Versus Primary Mach Number	46

Table No.		
1	Yaw and Pitch Forces	28
2	Side Force Calculation Parameters	47
3	Results of Yaw Side Force Calculations	48

RESEARCH AND DEVELOPMENT OF A VORTEX VALVE CONTROLLED HOT GAS (5500°F) SECONDARY INJECTION THRUST VECTOR CONTROL SYSTEM

by

T. W. Keranen

and

A. Blatter

Bendix Research Laboratories
Southfield, Michigan

SUMMARY

This program resulted in the successful demonstration of a vortex valve controlled secondary injection thrust vector control (SITVC) system on a solid propellant rocket motor. The vortex valves utilized in this program (Phase II) were developed during a Phase I effort.[1] These valves have the capability of modulating a 750 psia, 1 lb/sec flow of 16% aluminized, 5500°F solid propellant gas, with a demonstrated operating time of 50 seconds.

The rocket motor used for the test was the NASA-furnished EM-72 model, a 22-inch end burner containing 400 pounds of propellant. The motor is capable of producing approximately 6800 pounds of thrust with a mass flow rate of 30 lb/sec for 13 seconds.

The SITVC system consisted of a pilot stage which provided push-pull control of two SITVC hot gas vortex valves. The pilot stage contained a torque motor powered flapper-nozzle valve which, in turn, controlled two vortex amplifier valves. A 2000°F solid propellant gas generator (SPGG) supplied gas to the pilot stage. The two SITVC vortex valves were supplied with gas from an auxiliary 5500°F SPGG. The SITVC valves were installed on the horizontally positioned EM-72 rocket, such that one valve injected in the engine thrust nozzle vertical plane and the other in the horizontal plane.

The results of the hot gas tests conducted at Allegany Ballistics Laboratory, Cumberland, Maryland, in October 1967, showed that the vortex valve controlled SITVC System produced side forces up to 4% of the main engine thrust. The SITVC System materials and structure were able to control and handle the flow of aluminized 5500°F gas for over 50 seconds with little component degradation.

The technology resulting from this program definitely establishes the feasibility of utilizing vortex valves to control the injection of combustion chamber gases into a thrust nozzle. The demonstration of a buried nozzle rocket engine using vortex vlaves to control the injected flow should be the next stage in this development activity.

INTRODUCTION

Secondary Injection Thrust Vector Control Concept

The attitude of a rocket vehicle can be controlled by deflecting the main engine thrust vector. Thrust vector direction control can be provided by gimballing the thrust nozzle or by use of auxiliary movable vanes in the main nozzle exhaust. An alternate method of providing thrust vector control is by the technique known as Secondary Injection Thrust Vector Control (SITVC). The engine is stationary and fluid injected in the thrust nozzle deflects the rocket thrust gases to steer the vehicle. The fluid is injected into the thrust nozzle downstream of the nozzle throat (hence, the name "secondary injection"). Response is fast because the jets can be modulated rapidly in contrast to the mechanical method in which large engine masses are moved by servoactuators. The SITVC technique eliminates the need for complex seals and joints inherent in mechanical nozzle deflection systems.

A variety of fluids may be used for secondary injection, but it is most efficient to inject a high-temperature gas. The gas can be supplied from an independent source, or from the rocket motor. In the case of a direct chamber bleed system, the valves that control the secondary injection must withstand temperatures of 5000°F or more. In this severe environment, a fluidic device with no moving parts, such as a vortex valve, offers the possibility of greater reliability than a mechanical moving-part valve.

Some solid propellants are highly aluminized, and there is a tendency for molten aluminum oxide to condense out of the gas and to solidify and "plate out" on flow channel surfaces. This "plating out" of aluminum oxide can readily plug small clearances and passages, but the vortex valve, with its large passages and no-moving-part design, is less susceptible to plugging than conventional valve techniques.

A possible method of implementing a vortex valve controlled SITVC system on a buried nozzle solid propellant rocket engine is shown in Figure 1. The SITVC vortex valves will modulate bleed gas directly from the rocket motor combustion chamber and inject it in the nozzle for SITVC.

Program Description

The goal of this program was to demonstrate a vortex valve controlled SITVC system on a solid propellant rocket motor. This effort was conducted in parallel with the last part of the Phase I effort. The goal of the Phase I effort was the development and demonstration of a vortex valve to control the flow of hot gas. The basic approach of this program was to utilize existing NASA and Bendix technology and hardware. The program plan consisted of the following steps.

(1) Develop a system concept that will feature a two-axis, two vortex valve controlled SITVC system that will simulate a direct chamber bleed concept.

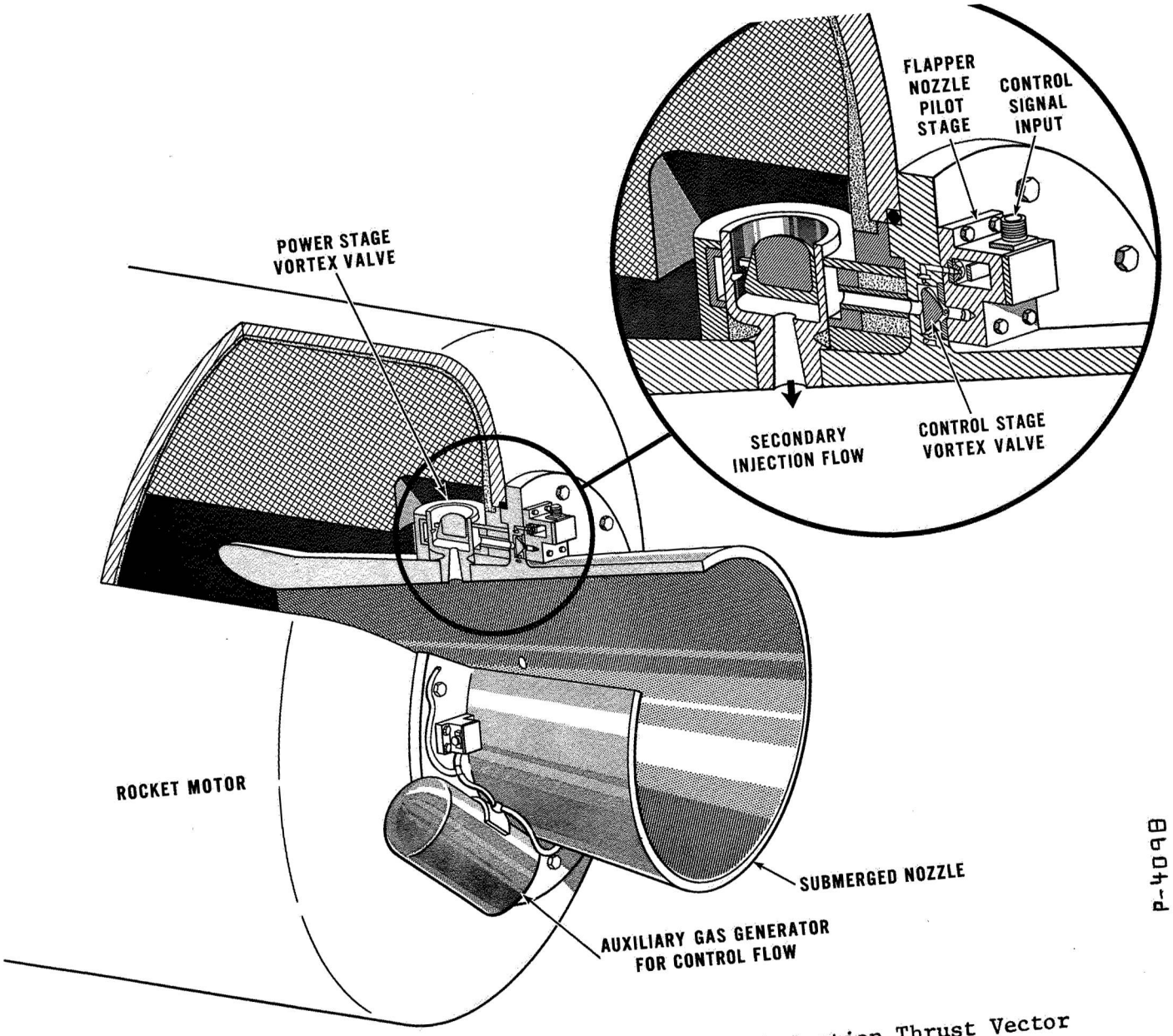

Figure 1 - Conceptual Vortex Valve Secondary Injection Thrust Vector Control System - Buried Nozzle Installation

(2) Design and fabricate a vortex valve controlled SITVC system that will utilize Phase I technology and hardware and the NASA supplied EM-72 rocket motor.

(3) Conduct a preliminary hot gas test on the fabricated hardware to evaluate system performance and structural integrity. This test was conducted as the sixth hot gas test reported in the Phase I final report.

(4) Conduct a complete system hot gas test on the EM-72 rocket motor at the Allegany Ballistics Laboratory, Cumberland, Maryland.

SITVC SYSTEM DESCRIPTION

System Operation

The system utilized for this program was a two-axis system with a single vortex valve in the yaw and pitch planes. The system is shown schematically in Figure 2.

The system included a rocket motor, a SITVC vortex valve main stage which modulated the flow of 5500°F gas, and a pilot stage which controlled the main stage. The main stage consisted of two vortex valves, such as that shown in Figure 3. These main stage valves were mounted on the EM-72 rocket motor such that one valve controlled secondary injection flow in the pitch plane and one in the yaw plane.

The main stage, which received its gas supply from a 5500°F solid propellant gas generator (SPGG), was operated in a push-pull mode. The push-pull mode of main stage operation was utilized to impart a constant impedance load on the 5500°F SPGG during system operation so that the SPGG would have a constant output flow rate. The main stage push-pull operation was such that when one vortex valve output flow decreased, the other vortex valve output flow increased a similar amount. The net result of this push-pull operation was that the total output flow from the two vortex valves is approximately constant.

The main stage system received control inputs from the pilot stage. The pilot stage consisted of two push-pull operated vortex amplifier valves which were controlled by a torque-motor flapper-nozzle valve. The pilot stage was supplied with gas from a 2000°F SPGG. The vortex amplifier valves were separated from the 2000°F SPGG by three subsonic orifices which provide the required pressure differentials between the vortex valve supply and control. The pilot stage operation was initiated by an electrical signal to the torque motor which produced a displacement of the flapper. The flapper displacement caused a reduction in flow through one of the nozzles and an increase in the nozzle upstream pressure. This increased pressure resulted in increased control flow to one of the vortex amplifier valves and a reduced output flow from that side of the pilot stage. This pilot stage vortex amplifier valve output flow was the control flow to the main stage vortex valve on that side of the system. Reduction of this control flow permitted an increase in the flow out of that main stage valve and an increase in the amount of rocket motor thrust vector deflection in the valve plane. Conversely, the other half of the system experienced a reduction in main stage valve flow and thrust vector deflection.

The SITVC system used for this program was designed as a heavyweight bench test model. An actual flyable vortex valve controlled SITVC system installed on a solid propellant rocket motor would be similar to the system shown in Figure 1. This type of system would not require an auxiliary 5500°F SPGG because the main stage vortex valves would be supplied directly

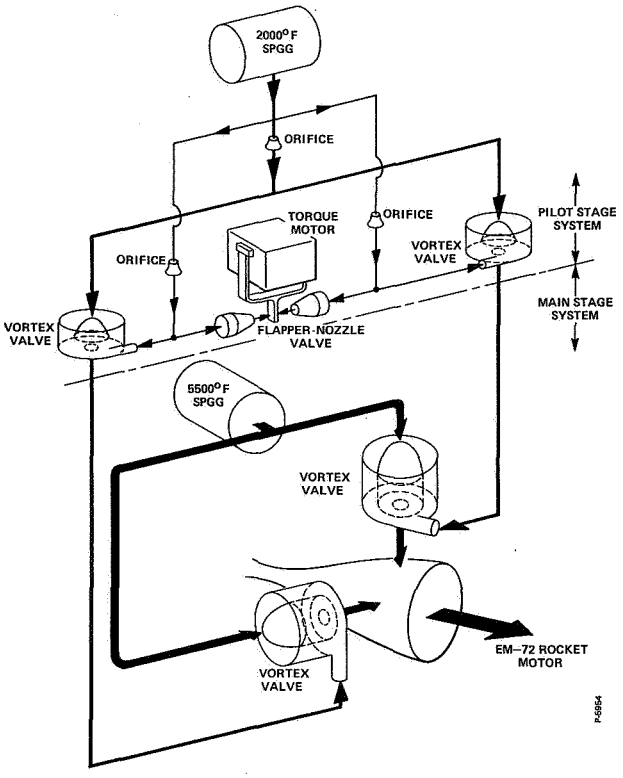

Figure 2 - Schematic of Vortex Valve Controlled SITVC System

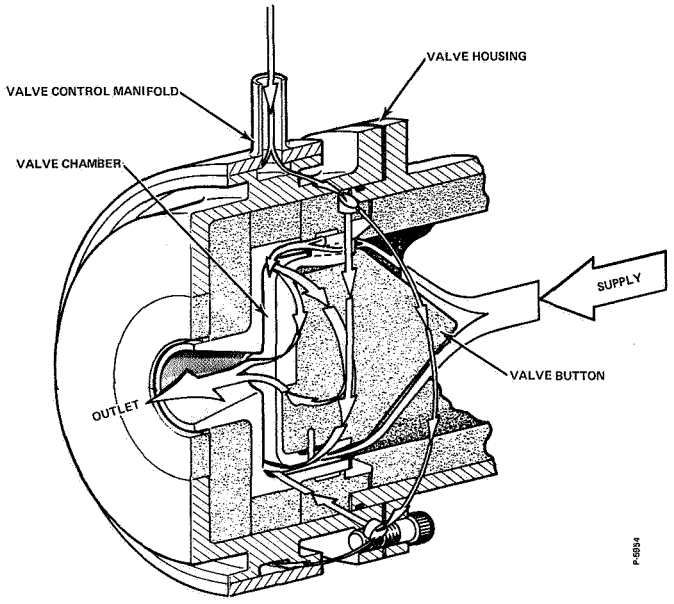

Figure 3 - 5500°F Vortex Valve

from the rocket motor. Also, in this system the main stage vortex valves would be independently controlled (not push-pull) and would normally be in the full turndown mode until thrust vectoring is commanded. When rocket motor thrust vectoring is required, the appropriate vortex valves or valve combinations would supply the proper amount of secondary injectant gas to obtain the desired thrust vector deflection. This technique will result in a SITVC system that is inherently simple and lightweight.

System Design

Installation of the vortex valve controlled SITVC system on the EM-72 rocket motor is shown in Figure 4 (also see Figures 15, 16, and 17). The direct chamber bleed buried nozzle concept was not used in this installation due to inherent design limitations of the rocket motor. The direct chamber bleed concept was simulated by supplying the SITVC valves from an auxiliary gas source via a plenum chamber.

The two SITVC vortex valves were placed in two axes; one in the yaw plane at 270 degrees and one in the pitch plane at 0 degree. Both of the valves were located on the nozzle divergent cone at 75% of the distance from the nozzle throat to the nozzle exit. Each injector port was surrounded by several pressure taps to measure the shape of the shock pattern and the pressure distribution in the nozzle at varying injectant flows. Two-plane single-point injection was incorporated because of the large volume manifolds on the 5500°F SPGG necessary for single-point injection. The single-point injection offered the possibility of isolating each vortex valve performance for test evaluation.

The two auxiliary SPGG's were mounted, as shown in Figure 4, to minimize the bends in the 5500°F gas manifolding and to minimize changes in torques on the engine and test stand assembly, during the test, due to change in SPGG masses.

Main stage SITVC vortex valves utilized in this program were developed during the Phase I effort. The valve configuration, showing basic dimensions and materials, is shown in Figure 5.

Hot gas flowing out of the main stage vortex valve was to be measured with a "weeping" orifice system. The "weeping" orifice system, shown in Figure 6, used a port in the vortex valve injection nozzle as a subsonic orifice. The port was flowed with nitrogen that passed through an upstream sonic orifice. The sonic orifice was sized to provide a constant nitrogen flow out of the port under all conditions, with the nitrogen source regulated at 2000 psia. A change in hot gas flow through the vortex valve load orifice caused a variation in impedance to the flow of nitrogen through the port. This variation in flow impedance produced a change in pressure upstream of the pressure port. This pressure variation was calibrated to provide the measurement of flow through the vortex valve.

The hot gas flow was introduced into a short plenum chamber outside the SPGG combustion chamber, and then directed to the SITVC vortex valves through two 5.0-inch diameter steel manifolds internally insulated with carbon phenolic insulation.

FOLDOUT FRAME

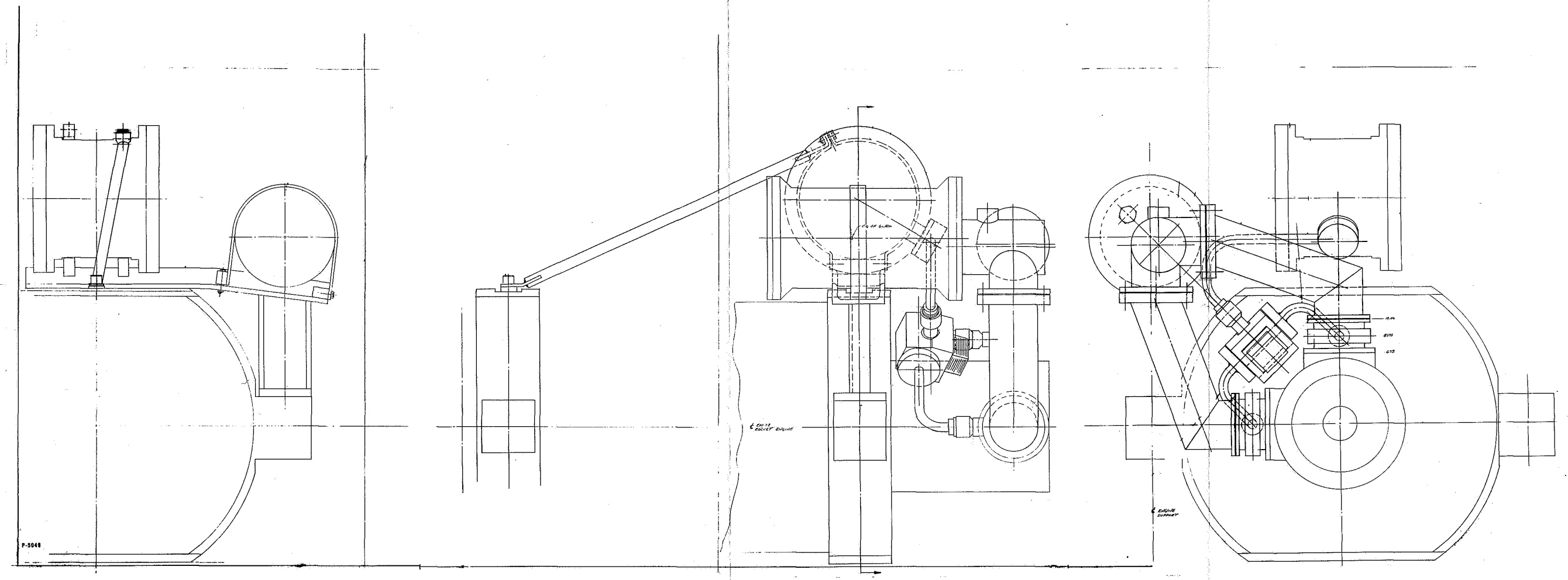

Figure 4 - Vortex Valve Installation on the EM-72 Rocket Motor Nozzle

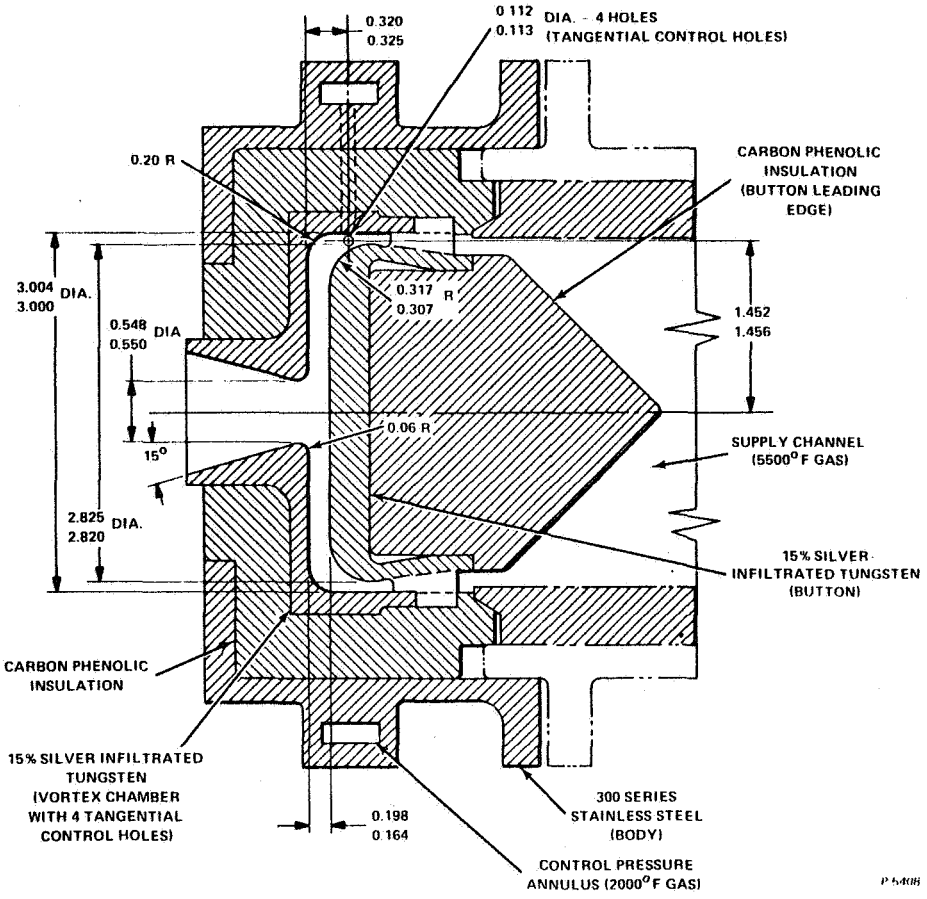

Figure 5 - 5500°F Vortex Valve Configuration, Basic Dimensions and Materials

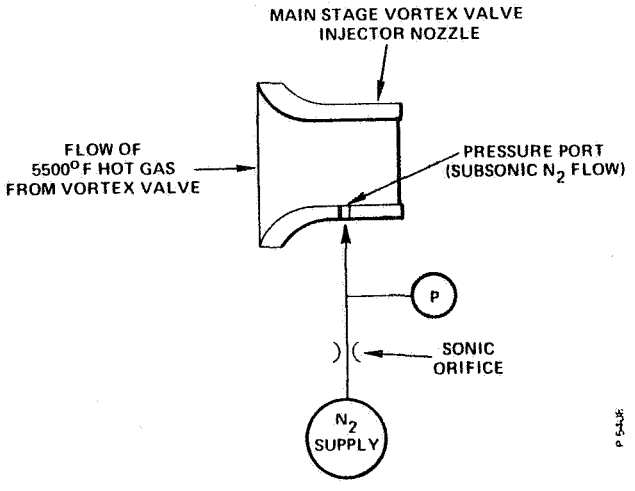

Figure 6 - Main Stage Vortex Valve Weeping Orifice Flow Measurement System

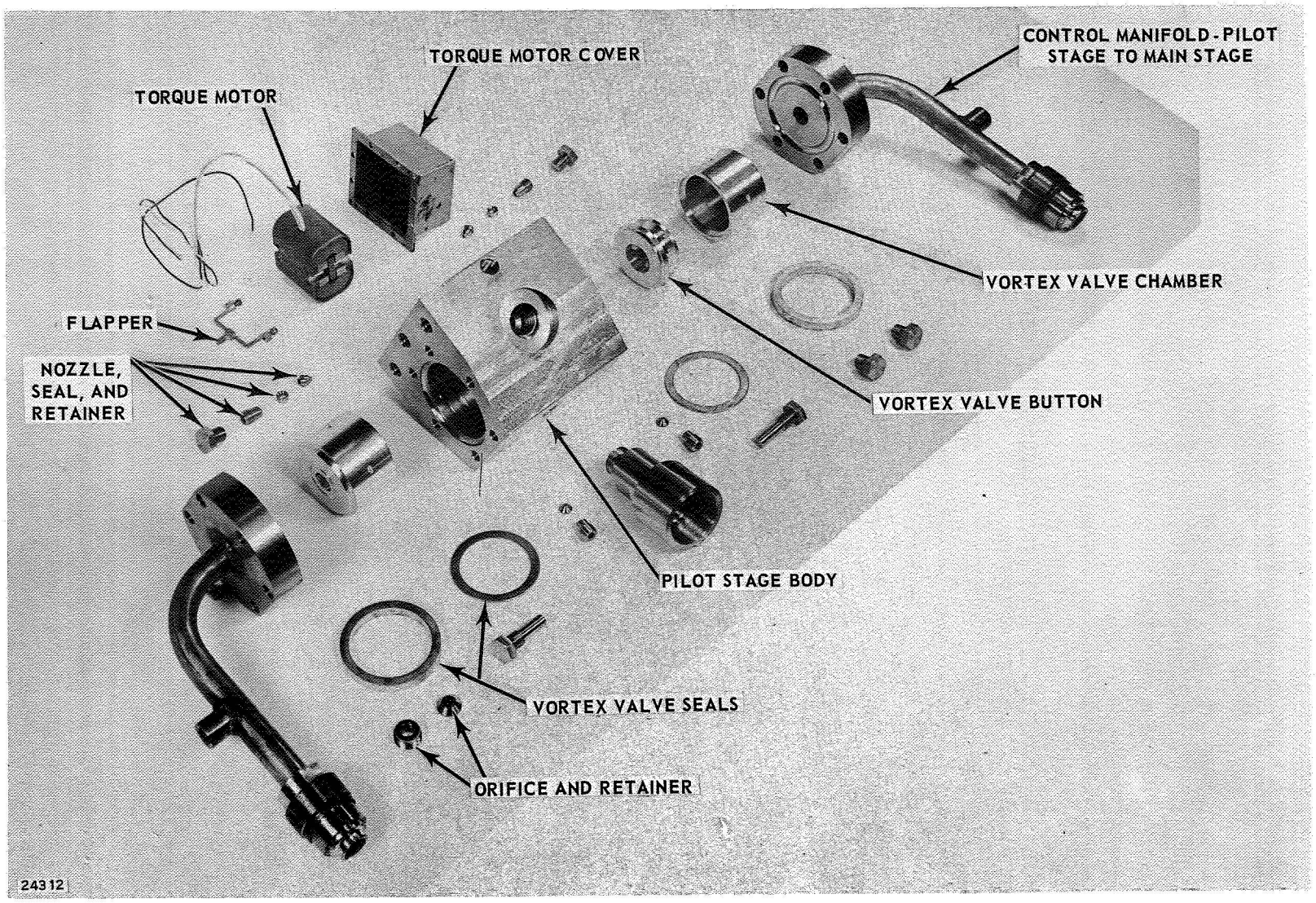

Figure 7 - Disassembled View of the 5500°F SITVC System Pilot Stage

The pilot stage 2000°F gas was supplied from a SPGG manufactured by Olin Mathieson Company. The propellant formulation was "OMAX 453D." Manifolding used in the pilot stage was made from RA 333 pipe (Rolled Alloy, Inc.).

Materials used in the pilot stage were: body-RA 333; orifices and vortex amplifier valves — TZM molybdenum; seals — copper. The pilot stage component parts are shown in Figure 7.

Rocket Motor and Test Stand Description

The rocket motor and test stand used for the test were supplied by a separately contracted effort between Hercules ABL and NASA. The EM-72 rocket motor is a 22-inch end burner containing approximately 400 pounds of propellant. The engine grain and nozzle were modified from an original design to produce approximately 30 lb/sec mass flow rate for a duration of approximately 13 seconds.

The test stand is designed for measuring engine yaw plane forces, pitch plane forces, and axial engine thrust. A schematic of the engine and test stand assembly is shown in Figure 8. The rocket motor, SITVC system, and test stand assembly had a calculated natural frequency of 20 hertz.

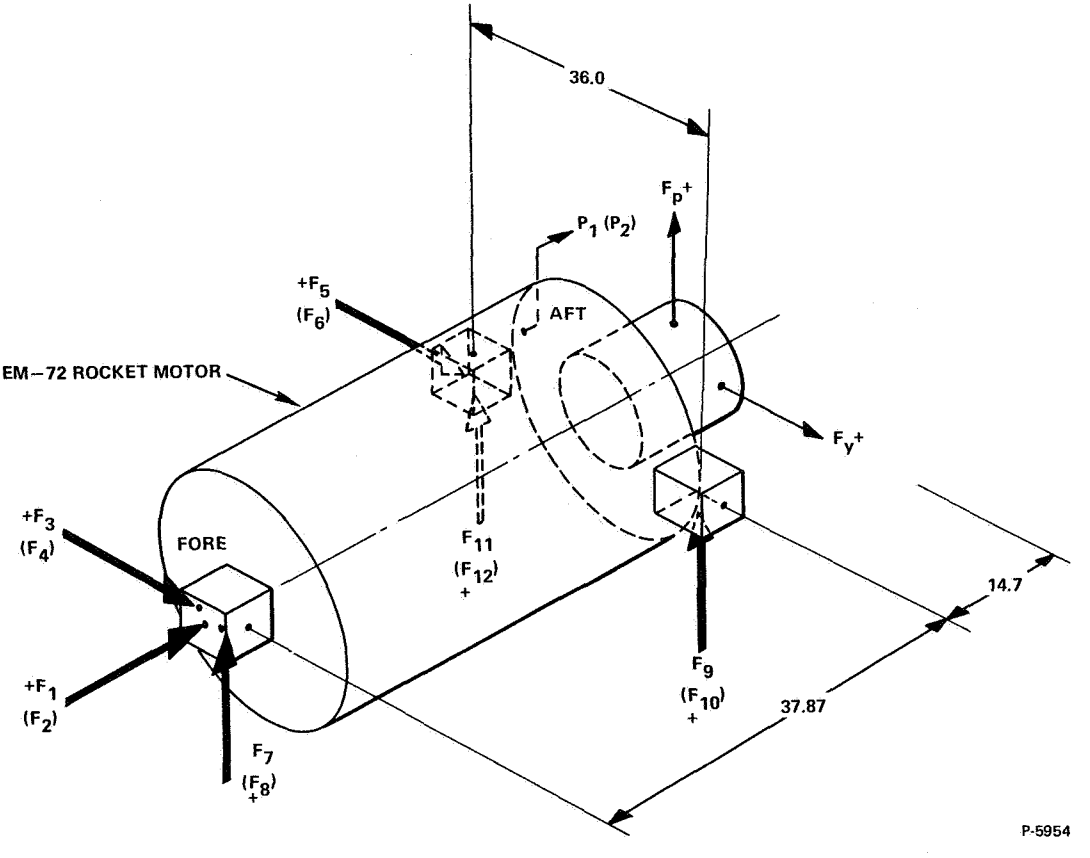

Figure 8 - Thrust Stand Transducer Locations

TEST RESULTS

The testing accomplished during this program was done in two parts. Cold gas test of the SITVC system and components was performed at the Bendix Research Laboratories test facilities to verify the predicted performance of the system and components prior to the hot gas test. The hot gas test of the SITVC system mounted on the EM-72 rocket motor was carried out at Allegany Ballistics Laboratory on 14 October 1967. Test objectives of the program were:

(1) Simulate a direct chamber bleed SITVC system and determine the effectiveness of vortex valve controlled injectant flow.

(2) Demonstrate the throttling efficiency of the vortex valve with the injectant flow.

(3) Demonstrate the capability of the vortex valve to reliably control the flow of 5500°F, highly aluminized gas.

Cold Gas Test Results

Cold gas testing was accomplished to determine the performance of the main stage SITVC vortex valves and the complete vortex control system before hot testing. The SITVC vortex valves were tested on gaseous nitrogen by regulating the supply flow pressure at 750 psig and increasing the control flow pressure from 750 psig to a level at which the supply flow was turned off. Resulting valve performance is shown in Figures 9 and 10.

Note the steep (high gain) portion of the turndown curve. Experience with vortex valves indicates that this portion of the turndown curve can be controlled by various geometric changes in the vortex valve. However, this portion of the curve is always steep, and as long as the valve turndown is proportional with control pressure, the valve geometry normally is not changed. The gain may be reduced by changes in the valve diameter ratio, the chamber length and spoilers on the chamber walls. Flow calibration curves are shown in Figure 11.

The test schematic and results of the SITVC system test cold gas test are shown in Figures 12 and 13. The cold gas tests indicated that the SITVC system should function as intended during the hot gas test.

Hot Gas Test Results

The hot gas system test schematic is shown in Figure 14. The arrangement of the vortex valve SITVC system components and the location of the various pressure transducers are shown. The transducers were installed in pairs for redundancy in practically all cases. Note that the lower portion of the circuit (the dashed lines) is the "weeping" orifice flow measuring method used to determine the hot gas injectant flows. Pictures of the system installation prior to the hot gas test are shown in Figures 15, 16, and 17.

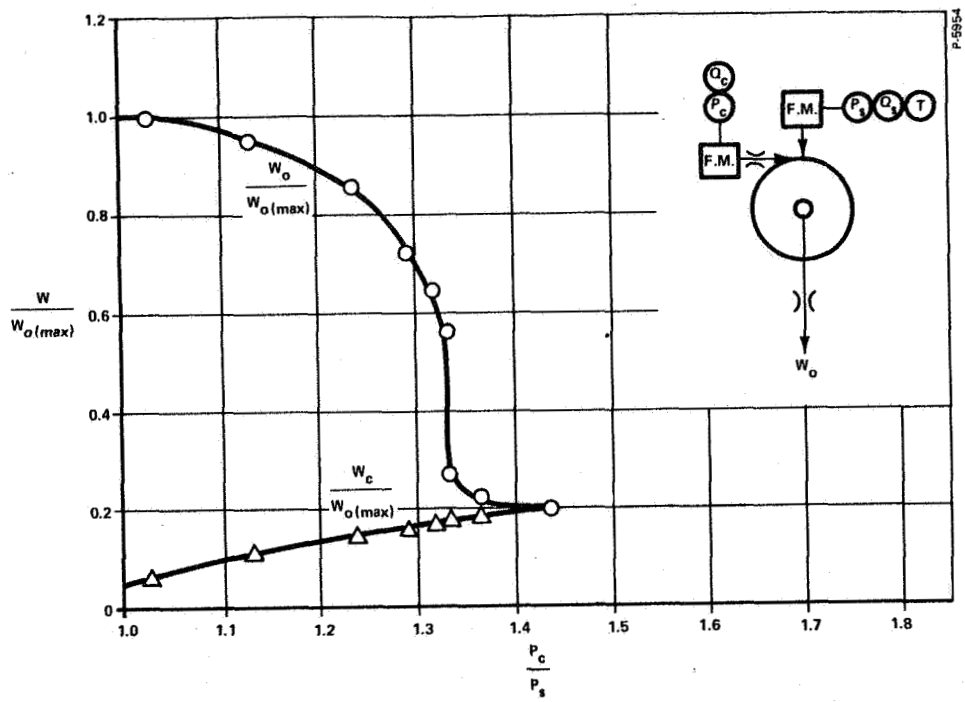

Figure 9 - Main Stage SITVC Vortex Valve No. 1 - Cold Gas Turndown Performance

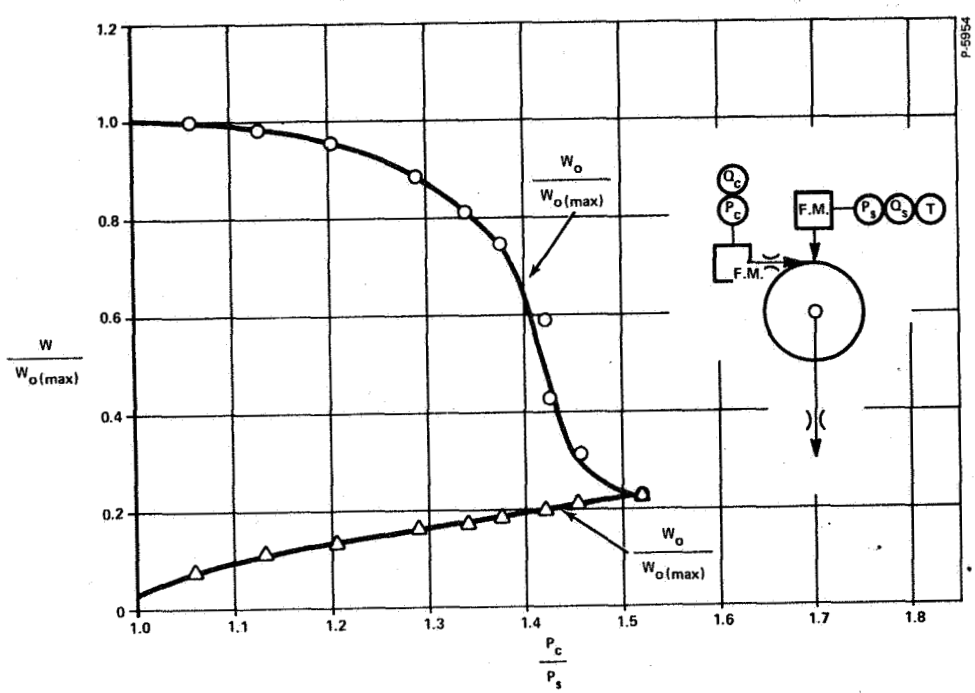

Figure 10 - Main Stage SITVC Vortex Valve No. 2 - Cold Gas Turndown Performance

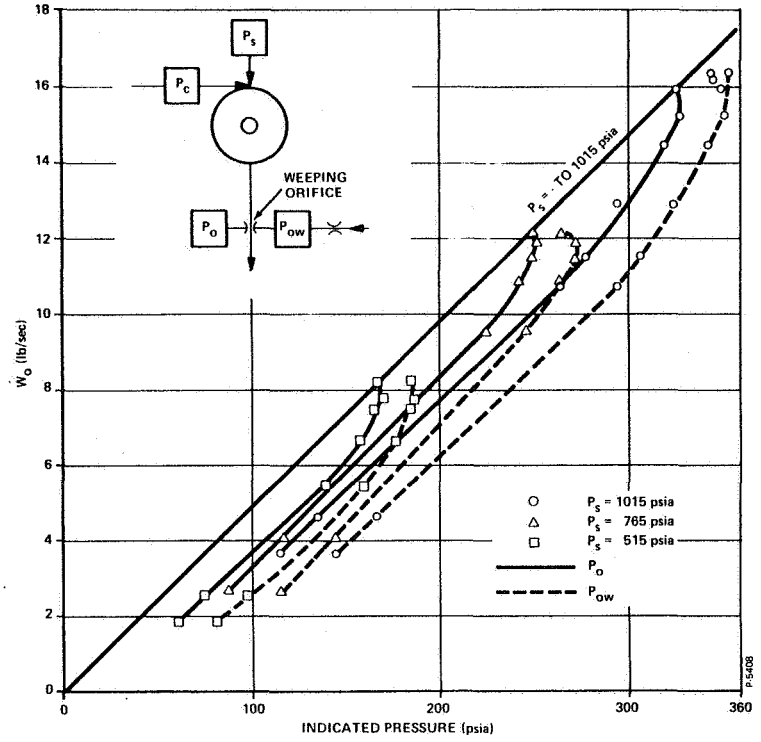

Figure 11 - Pressure Tap and Weeping Orifice Cold Gas Flow Calibration (Corrected to Hot Gas Flow)

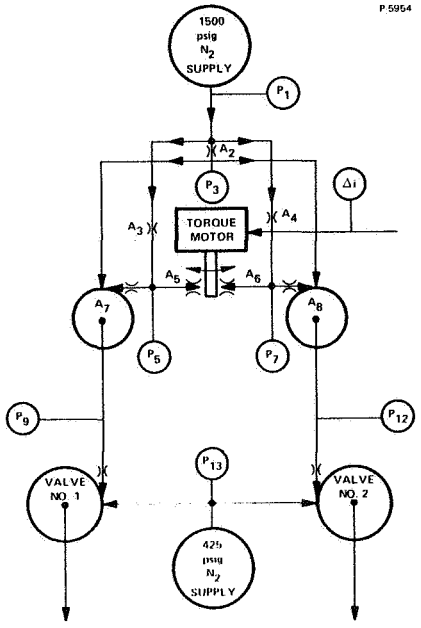

Figure 12 - Test Schematic for Cold Gas Test of the SITVC System

	P_1 psia	P_{13} psia	P_3 psia	P_5 psia	P_9 psia	P_7 psia	P_{12} psia	Input Signal
Design Value	2600	750	1515	1590–2050	789–1125	1590–2050	787–1125	
Test Data Projected Data	1510 2600	430 746	935 1620	905–1115 1568–1933	435–645 754–1118	945–1215 1638–2105	455–615 788–1065	±150 Ma 1 hertz sine wave
Test Data Projected Data	1495 2600	428 745	935 1625	900–1120 1565–1948	435–635 757–1117	935–1205 1625–2095	445–615 774–1070	5 hertz sine wave
Test Data Projected Data	1500 2600	430 745	935 1620	895–1140 1551–1975	445–620 772–1075	935–1200 1620–2080	443–595 768–1032	10 hertz sine wave
Test Data Projected Data	1500 2600	432 749	935 1620	925–1125 1603–1950	455–610 788–1057	935–1200 1620–2080	455–580 788–1005	15 hertz sine wave
Test Data Projected Data	1500 2600	433 752	945 1637	935–1135 1620–1968	470–595 814–1031	950–1200 1646–2080	455–570 788–988	20 hertz sine wave
Test Data Projected Data	1512 2600	435 748	945 1625	910–1175 1565–2020	435–650 739–1118	910–1215 1565–2090	455–625 782–1075	1 hertz sawtooth wave
Test Data Projected Data	1495 2600	432 751	905 1575	895–1175 1558–2045	435–635 757–1105	905–1205 1574–2095	445–623 773–1083	1 hertz square wave full amp
Test Data Projected Data	1480 2600	420 738	905 1590	895–1035 1572–1820	435–615 764–1080	950–1135 1670–1995	445–580 782–1020	1 hertz square wave 2/3 amp
Test Data Projected Data	1470 2600	415 734	905 1600	925–980 1635–1735	465–585 823–1035	975–1050 1725–1860	450–520 796–920	1 hertz square wave 1/3 amp

P-5954

Figure 13 - SITVC System Cold Gas Test Performance

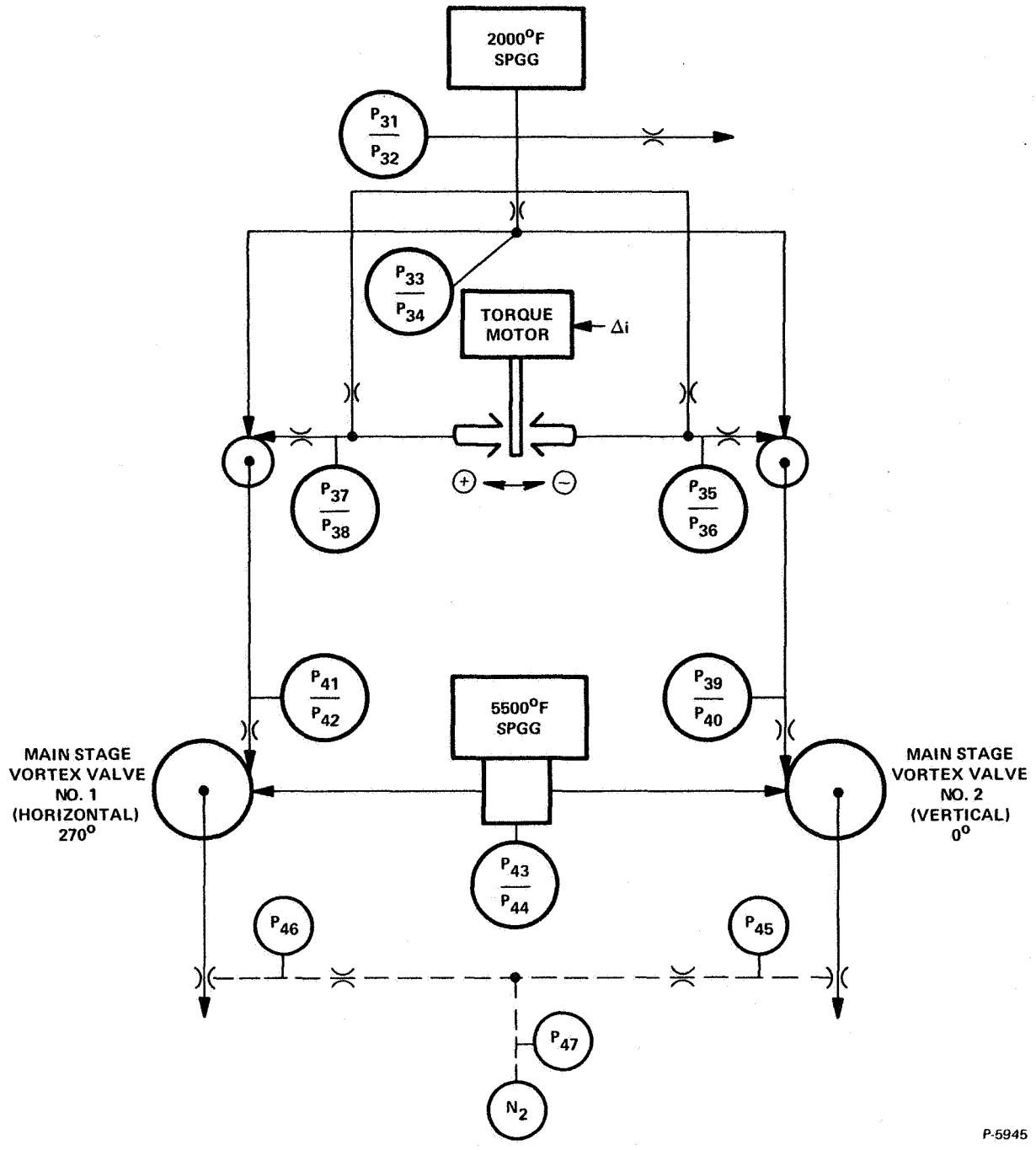

Figure 14 - Schematic of Hot Gas Test System

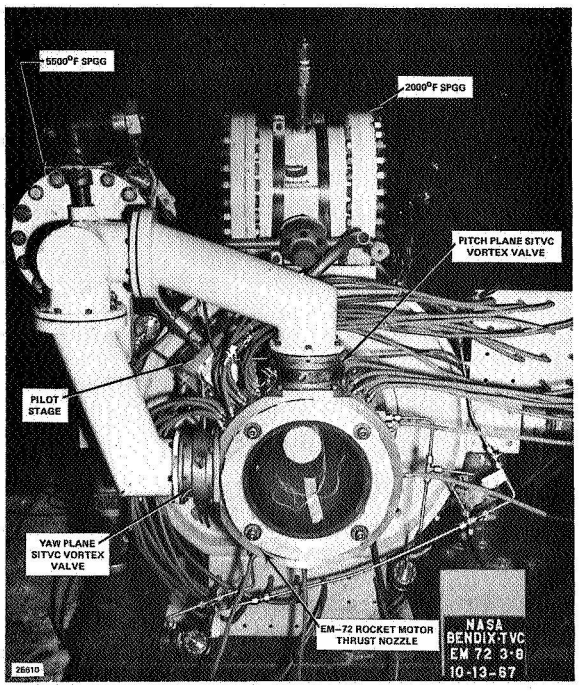

Figure 15 - Vortex Valve Controlled SITVC System Installation on EM-72 Rocket Motor - Component Location

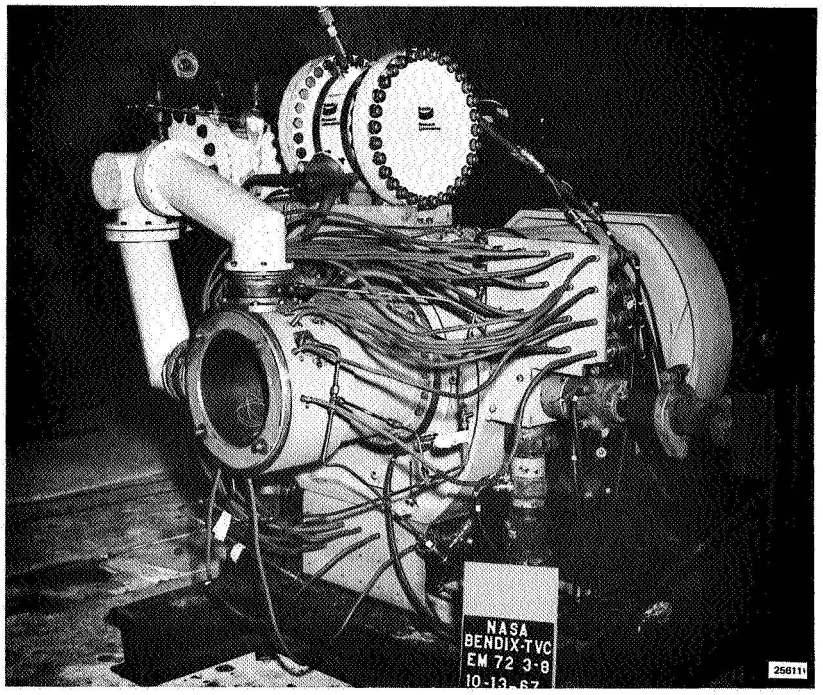

Figure 16 - Vortex Valve Controlled SITVC System Installation on EM-72 Rocket Motor - Side View

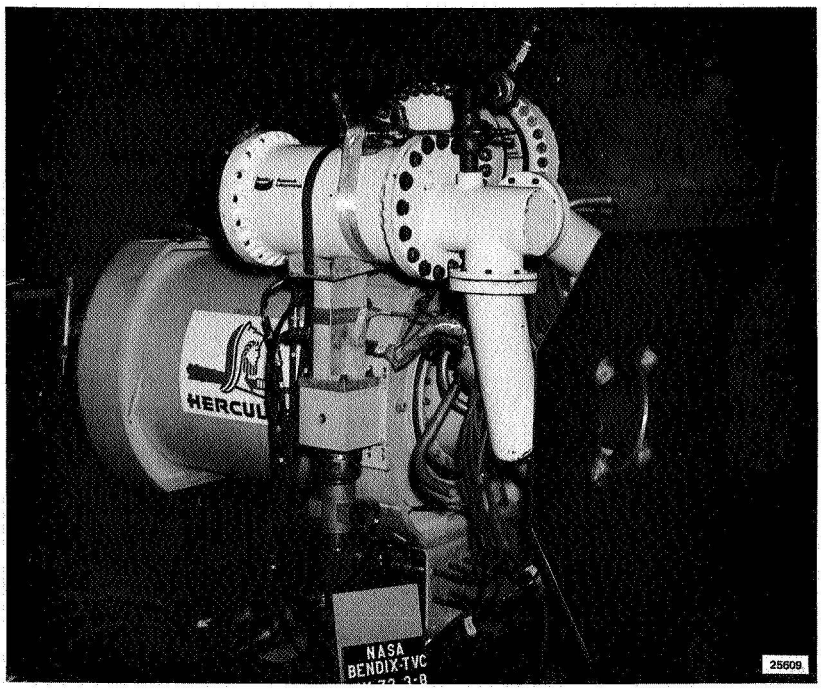

Figure 17 - Vortex Valve Controlled SITVC System Installation on EM-72 Rocket Motor - Side View

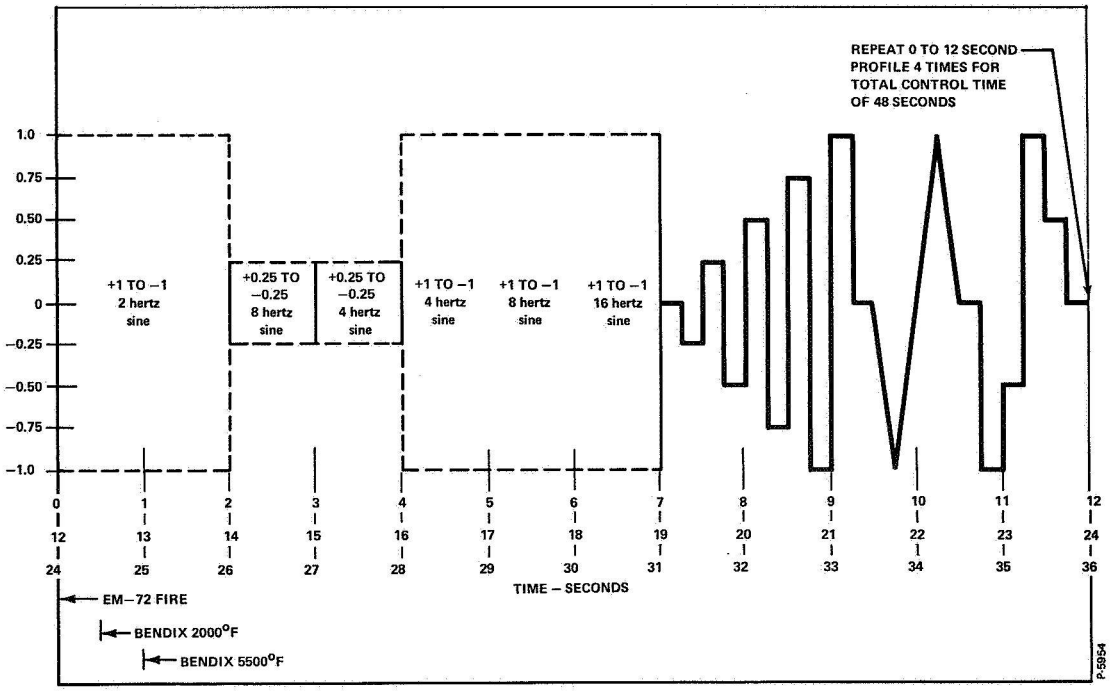

Figure 18 - Vortex Valve SITVC System Duty Cycle for EM-72 Rocket Motor and Bendix Controls

The effective test duty cycle, which matched the EM-72 rocket motor burning time, is shown in Figure 18. This duty cycle was sequentially repeated four times during the burn time of the 5500°F SPGG. The expected burn time of the EM-72 rocket motor was 12 seconds; the 5500°F SPGG, 45 seconds; and the 2000°F SPGG, 32 seconds.

Prior to the test, all pressure and force transducers were calibrated and checked. Also, several dry runs were performed to check out the firing circuits, the TVC input program, the data acquisition system, and the various ancillary equipment.

Performance of the EM-72 rocket motor, the 5500°F SPGG, and the 2000°F SPGG during the test is shown in Figures 19, 21, and 22 as plots of operating pressure versus time. The rocket motor axial thrust for the test duration is shown in Figure 20. Test data show that the EM-72 rocket motor operated at an average pressure of 481 psia which was 60 psi lower than predicted. The engine produced a maximum axial thrust of 6800 pounds, which was 200 pounds lower than anticipated. The reduction in thrust and engine chamber pressure has no significant effect on the evaluation of the vortex valve control system.

The 2000°F SPGG, which provided control gas for the SITVC vortex valves, operated at an average pressure of 2200 psia during the initial 16-second period. As shown in Figure 21, the generator burned regressively from 10 seconds until burnout. No external reason, such as leaks, has been found to account for the regressive burning. The design pressure was 2600 psi. The 5500°F SPGG which produced the secondary injectant gas operated at an average pressure of 540 psia during the initial 16-second period. Note that this SPGG burned progressively throughout the run. The design pressure for this generator was 750 psia. Although both SPGGs operated at lower pressures than intended, the control system generated P_c/P_s ratios up to 1.8 to 1. This pressure ratio should have been enough to turn down the main stage vortex valves. The injectant flow would be reduced by the lower 5500°F SPGG pressure but this would not effect the final test conclusions.

The measured pressures in the SITVC system at test times of 4.3, 12, 24, and 28 seconds, are shown in Figures 23 through 26. Test data indicated that the pilot stage began malfunctioning at approximately 16 seconds and ceased functioning at 23.6 seconds. The pilot stage malfunction appears to have been caused by failure of the torque motor that powered the pilot stage flapper-nozzle valve.

During the first 16 seconds of the test, the SITVC system operated as intended, except for the low system pressures. The "weeping orifice" flow measurement system did not provide data. Control pressure-to-supply pressure ratios for the pilot stage vortex valves and the SITVC vortex valve remained fairly uniform during the first 16-second interval. The

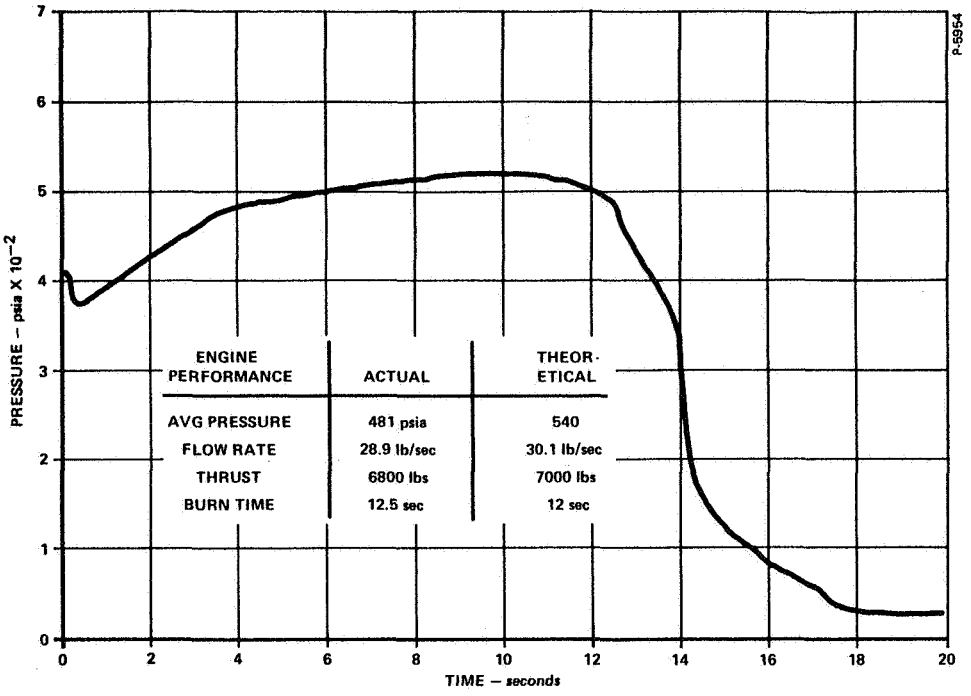

Figure 19 - EM-72 Rocket Motor Operating Pressure

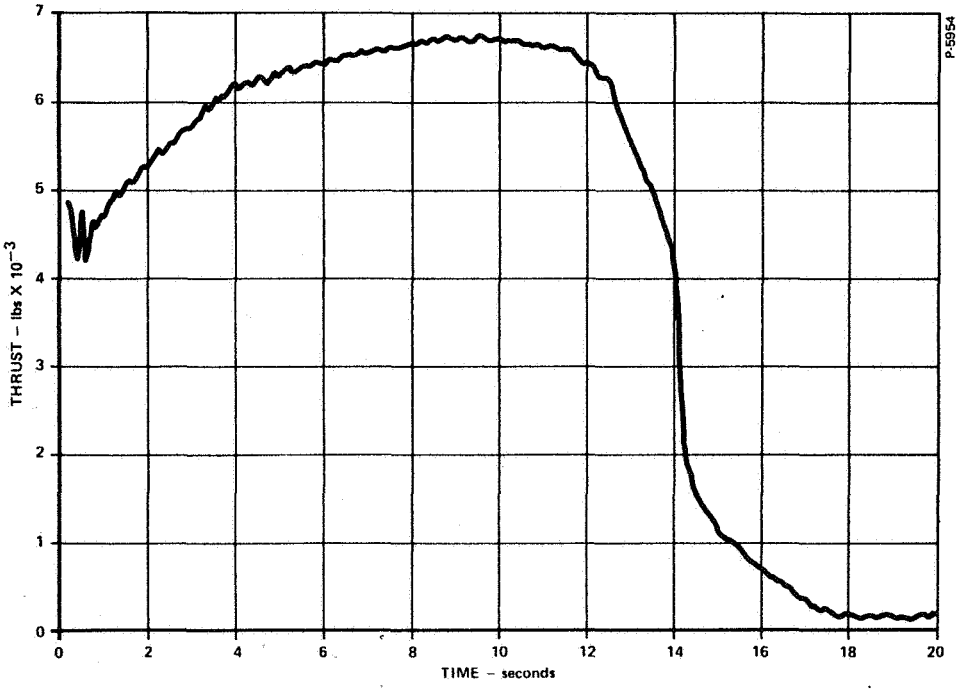

Figure 20 - EM-72 Rocket Motor Axial Thrust

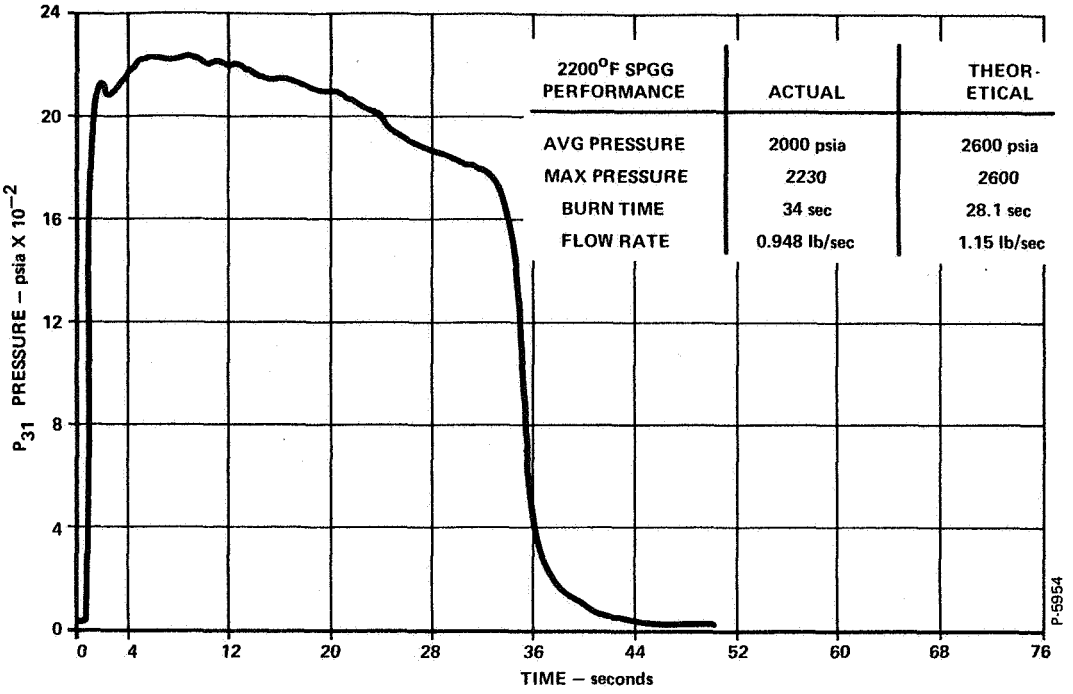

Figure 21 - 2000°F SPGG Operating Pressure

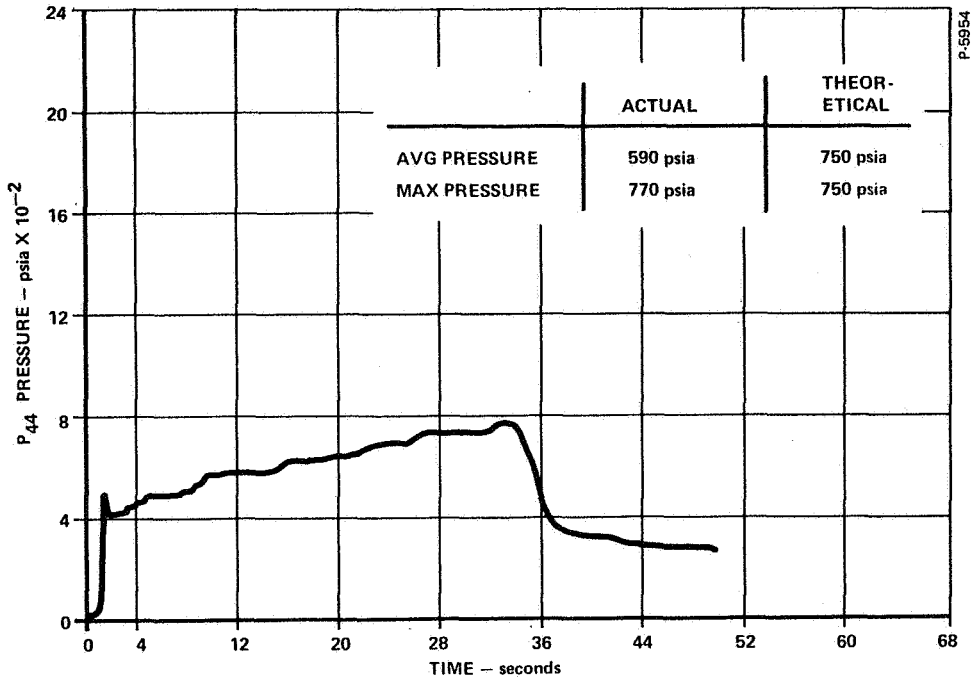

Figure 22 - 5500°F SPGG Operating Pressure

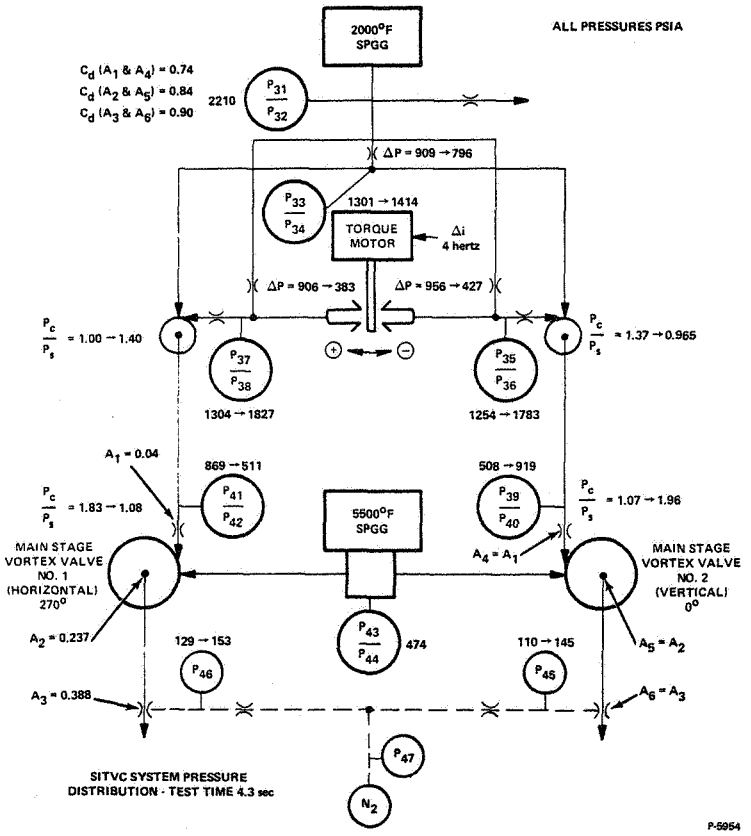

Figure 23 - SITVC System Pressure Distribution — Test Time 4.3 Second

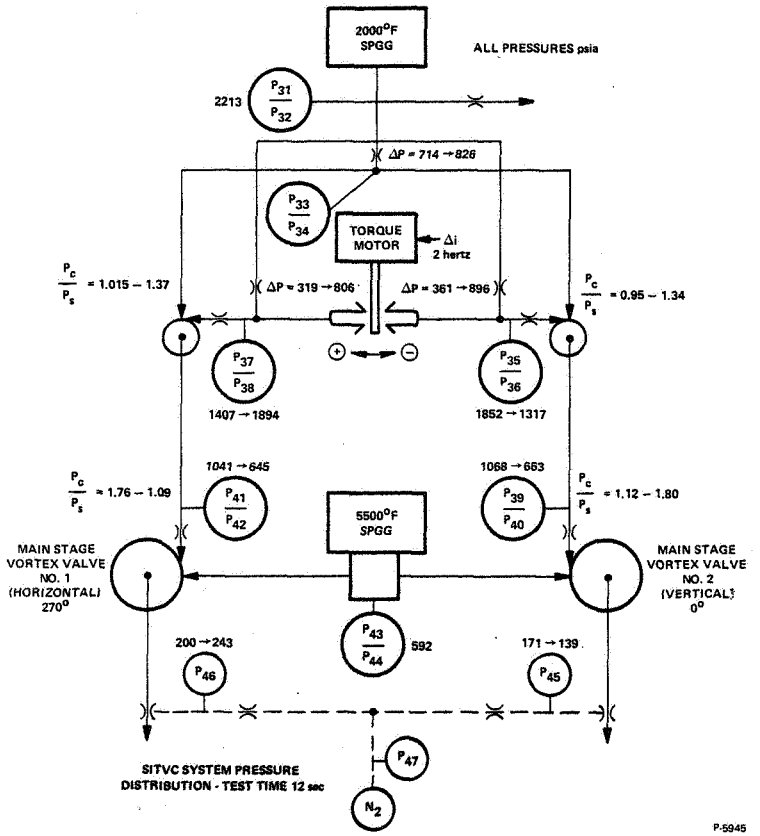

Figure 24 - SITVC System Pressure Distribution — Test Time 12 Second

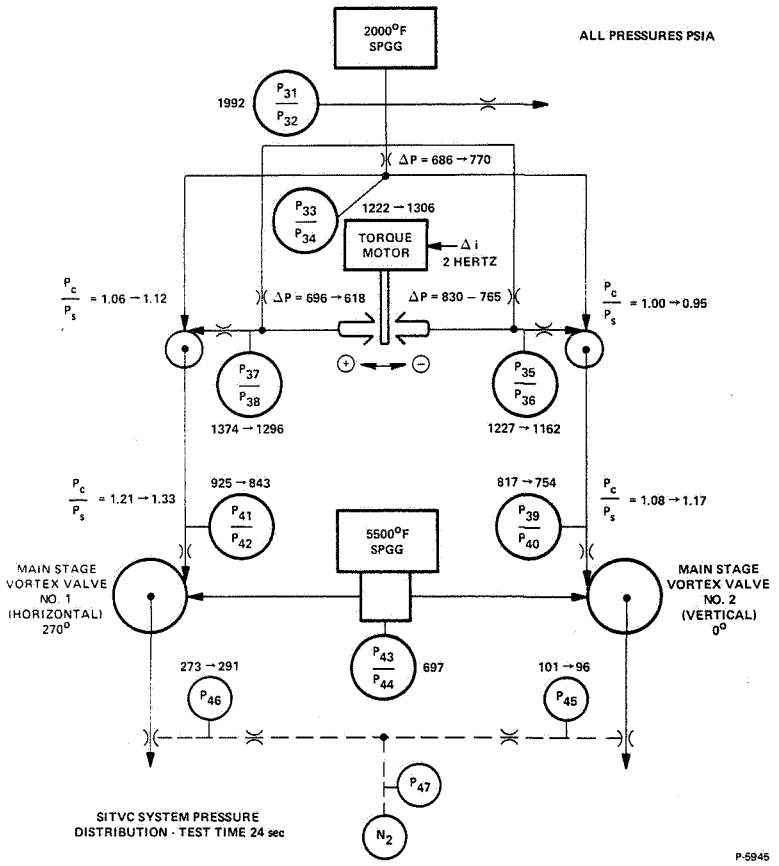

Figure 25 - SITVC System Pressure Distribution - Test Time 24 Second

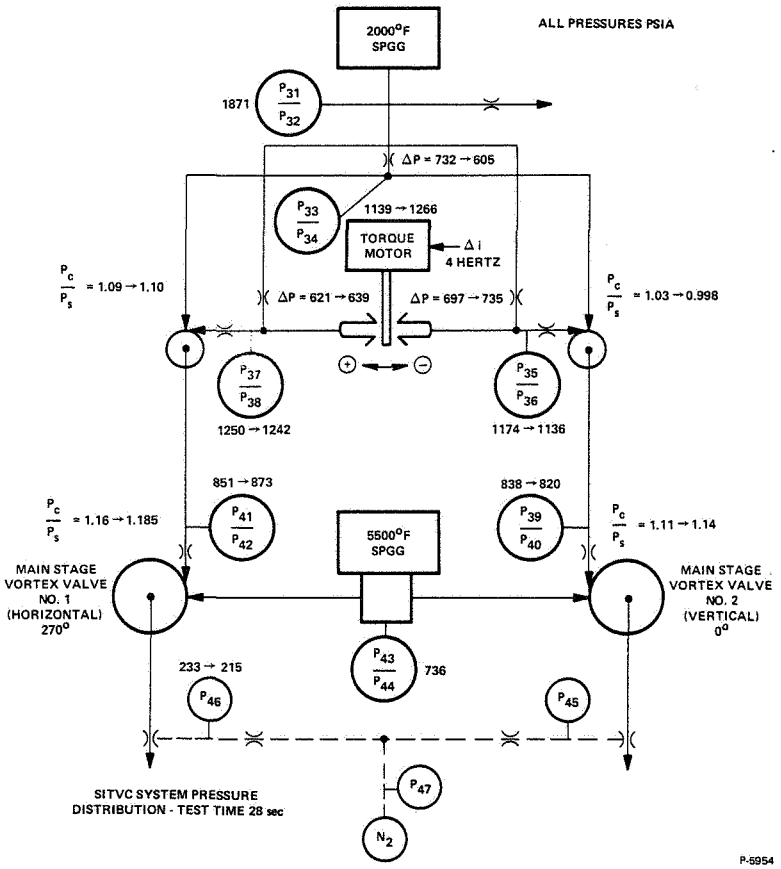

Figure 26 - SITVC System Pressure Distribution - Test Time 28 Second

test P_c/P_s ratios for the yaw side vortex valves at test time 4.3 seconds, as compared to cold gas test results and calculated values, are shown below:

	P_c/P_s Yaw SITVC Vortex Valve	P_c/P_s Yaw Pilot Stage Vortex Valve
Hot Gas Data	1.08 to 1.83	1.00 to 1.40
Cold Gas Data	1.01 to 1.50	1.01 to 1.30
Theoretical	1.05 to 1.50	1.05 to 1.35

These figures are typical of the yaw and pitch sides of the system for the first 16 seconds of the test.

The "weeping orifice" flow measurement system failed to function. Pressures P_{46} and P_{45} did not vary with changes in valve flow as had been experienced in previous hot gas tests. Typical "weeping orifice" test data are shown in Figure 27. Failure of the flow measurement system to function was attributed to aluminum oxide from the hot gas alternately plugging and unplugging the sensing port. Loss of the flow measuring system resulted in no accurate measurement of SITVC vortex valve flow data and flow turndown performance.

One additional problem encountered in the SITVC system pilot stage was an instability condition that occurred at null and low amplitude inputs commands to the pilot stage flapper. Results of this flapper instability are represented in plots of pilot pressures P_{35} and P_{37}, shown in Figure 28. These pressures were controlled by the flapper position and became noisy for all null and low amplitude command signals. This noise condition occurred during the cold gas testing and was corrected to satisfy cold gas conditions by enlarging the flapper-nozzle vent area to the maximum possible in the existing hardware design. It was not known until after the hot gas test that the change was insufficient for the hot gas conditions.

The secondary injection side forces produced by the vortex controlled SITVC system on the EM-72 rocket motor are shown in Figures 29 through 32. These figures show test data for system command signals of 2, 4, 8, and 16 hertz. The main engine bias forces were obtained by the offset when the main engine fired but before the SITVC SPGG's fired. The average yaw and pitch forces obtained from the data were as shown in Table 1.

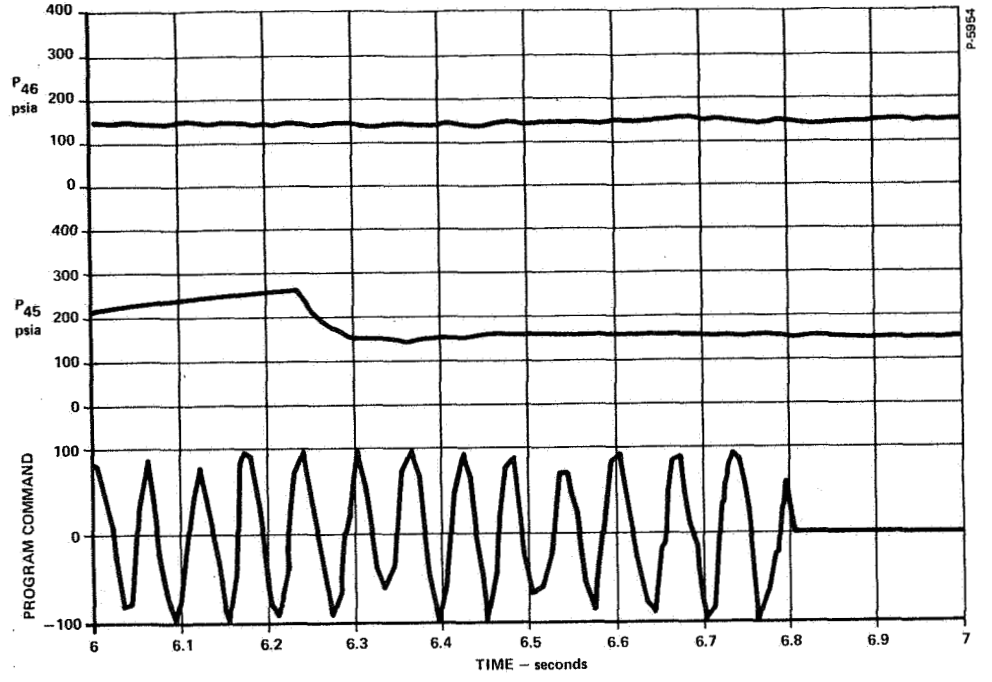

Figure 27 - SITVC Vortex Valve Weeping Orifice Flow Measurement Pressures P45 and P46

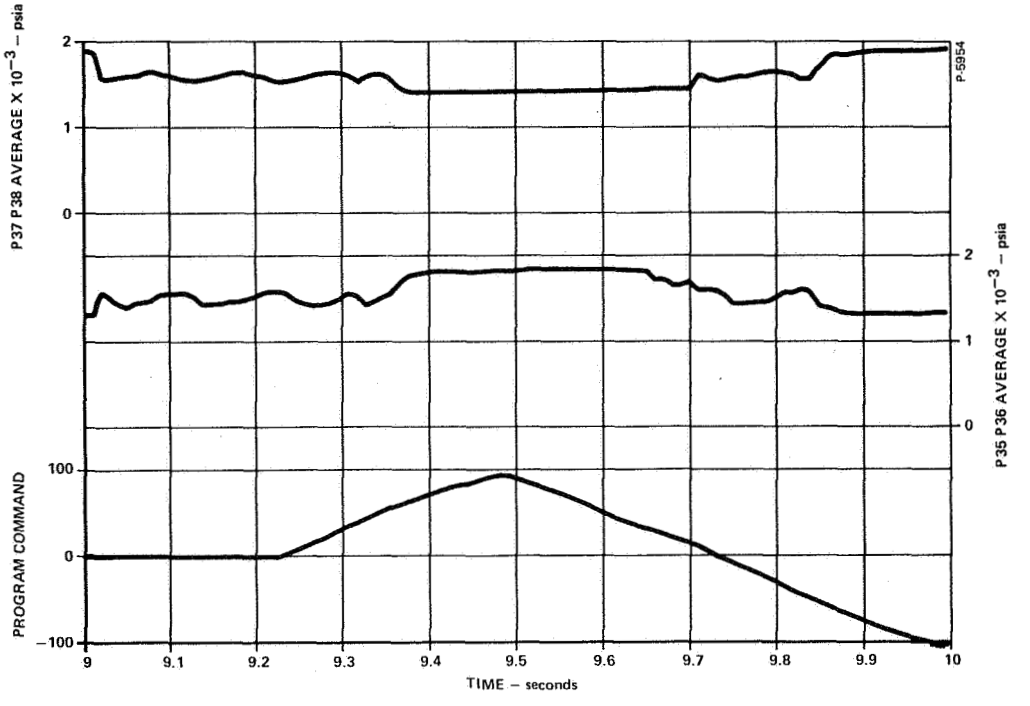

Figure 28 - Pilot Stage Pressures P35 and P37

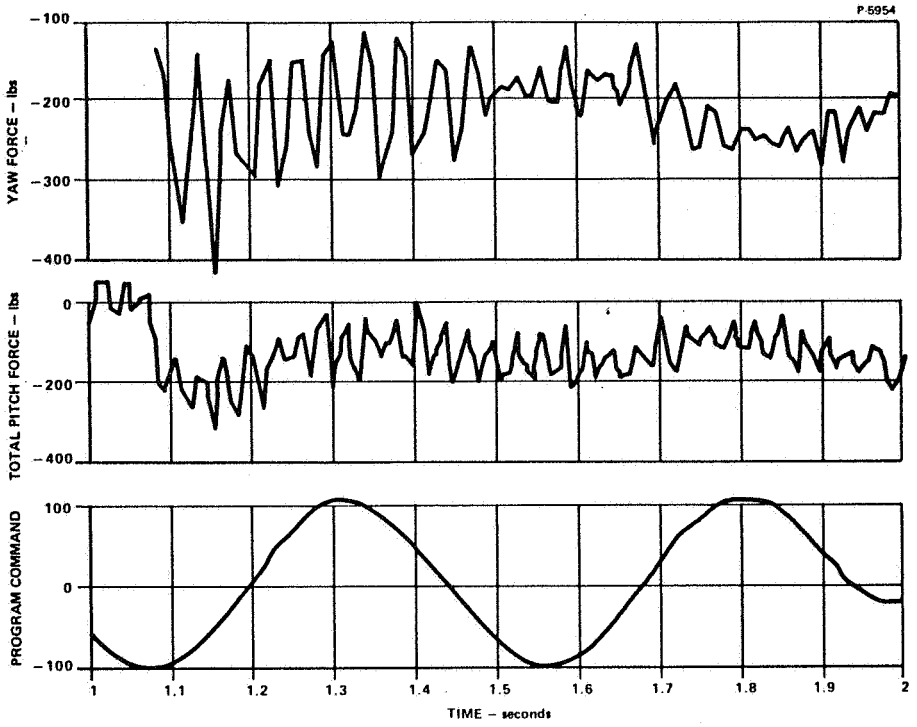

Figure 29 - EM-72 Rocket Motor Yaw and Pitch Forces - Command Input 2 Hertz

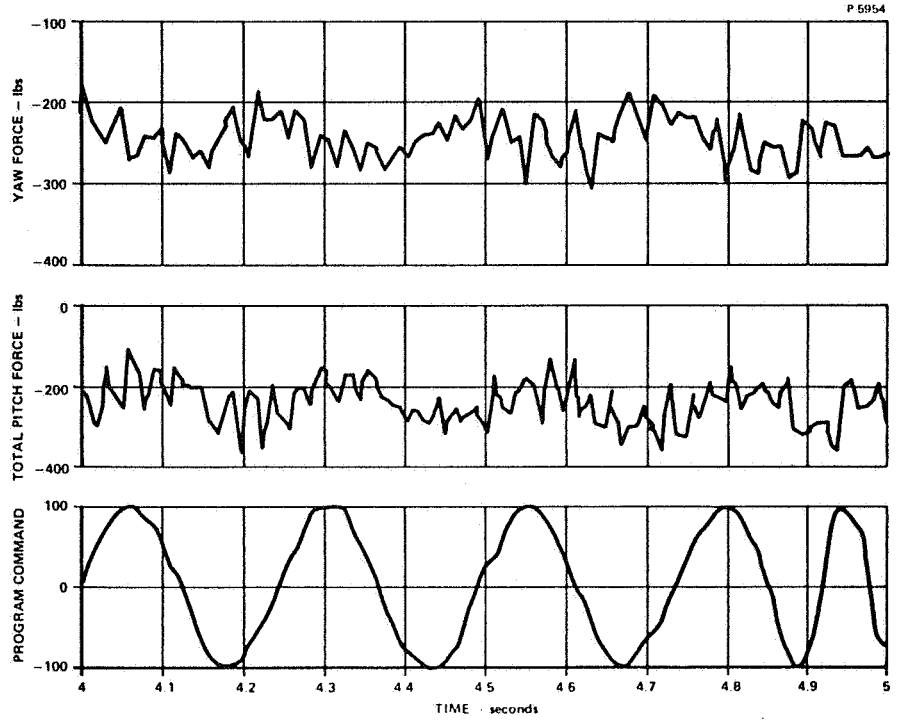

Figure 30 - EM-72 Rocket Motor Yaw and Pitch Forces - Command Input 4 Hertz

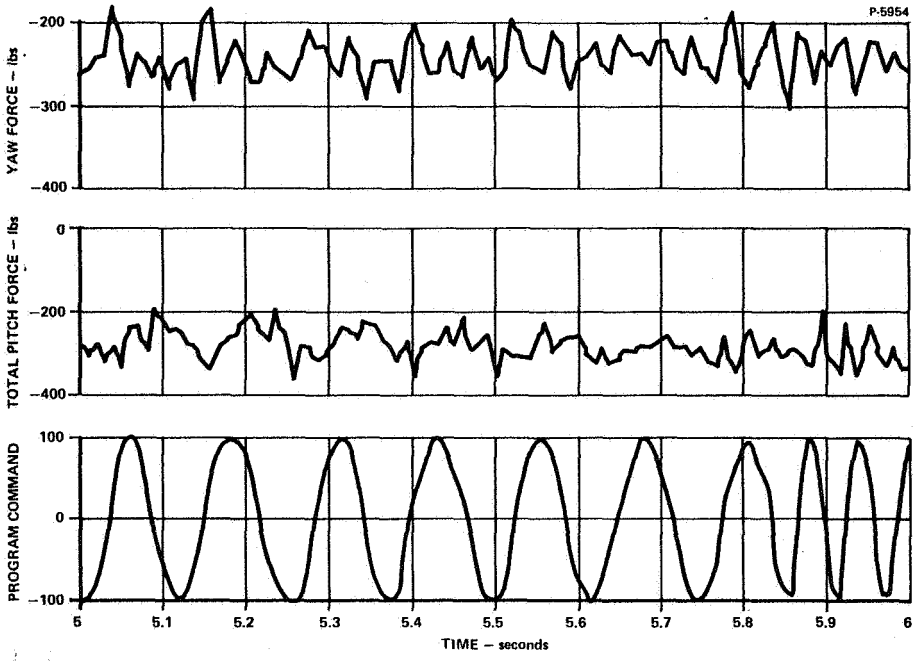

Figure 31 - EM-72 Rocket Motor Yaw and Pitch Forces - Command Input 8 Hertz

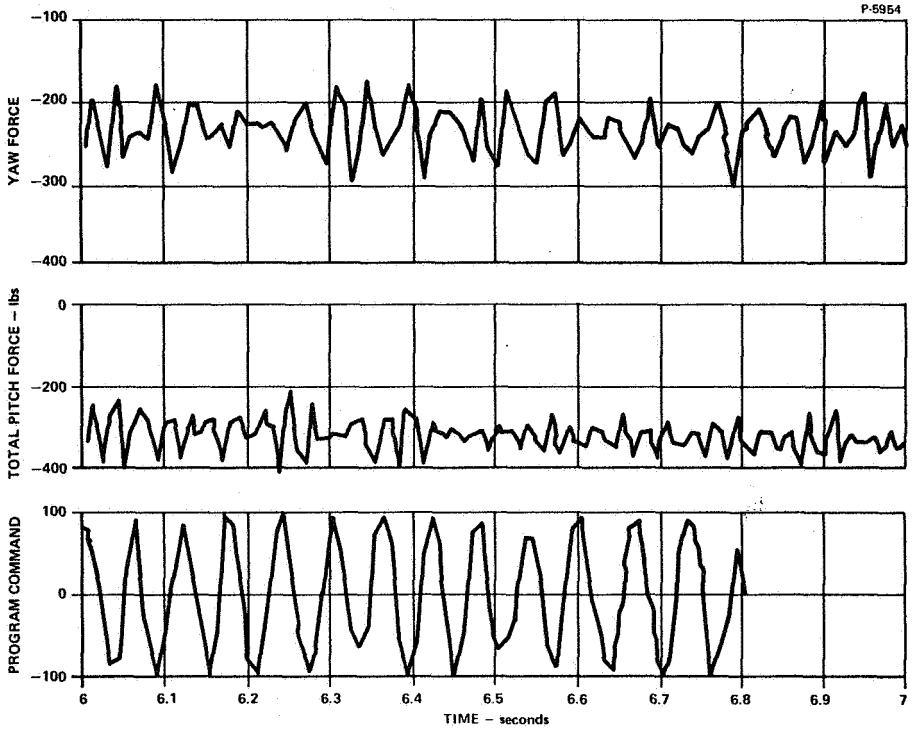

Figure 32 - EM-72 Rocket Motor Yaw and Pitch Forces - Command Input 16 Hertz

Table 1 - Yaw and Pitch Forces

Command Signal	Test Time	Total Yaw Force	Yaw Bias	Actual Yaw Force	Total Pitch Force	Pitch Bias	Grain Weight Loss	Actual Pitch Force
2 hz	1 - 2	175/260	-30	145/230	90/160	+40*	-47**	83/153
4 hz	4 - 5	216/269	-30	186/239	194/295		-140	94/195
8 hz	5 - 6	226/259	-30	196/229	253/302		-172	121/170
16 hz	6 - 7	(Noise)	-30	-	300/340		-201	139/189

*Pitch bias at beginning of test. Bias variation in latter part of test estimated from propellant consumption.

**Grain weight loss estimated from average burn rates of all three grains.

Due to the loss of the secondary injection flow data, it is difficult to perform a complete correlation between observed side force and theoretical side forces. Although the minimum injectant flow is not known, the maximum flow can be estimated. No vorticity is present at maximum flow conditions through a vortex valve; therefore, the flow may be estimated by using a simple multiple orifice in series analysis. The engine bias and maximum side force are known and a comparison of actual to theoretical force can be performed with reasonable confidence at these points.

Performing such an analysis and plotting the points for theoretical and actual performance on a graph of normalized side force versus normalized injectant flow results in Figure 33. The theoretical points agree well with the upper limit of the performance band associated with hot gas secondary injection. The point "actual side force at zero vorticity" is well within the expected band for hot gas. The computation of the points as an iterative process and a sample calculation is presented in appendix A. It appears that some loss in performance is present; however, the uncertainty of the injectant flow rate prevents drawing a conclusion regarding the effect of injectant jet rotation. The vortex valve will inject a rotating stream of fluid into the thrust nozzle at all times except when the vortex valve is full open. At this time there is no vorticity in the valve and the injected fluid will have no rotational component.

Note in Figure 33 that some side force exists at full turndown. This is caused by the control flow required by the vortex valve which enters the primary nozzle flow,thereby creating some side force. The supply flow to the vortex valve is zero at full turndown but control flow is maximum. As shown in Figure 1, if two vortex valve controlled injection ports are located 180 degrees apart in a thrust nozzle, the net thrust vector angle is still zero even though both valves are admitting control

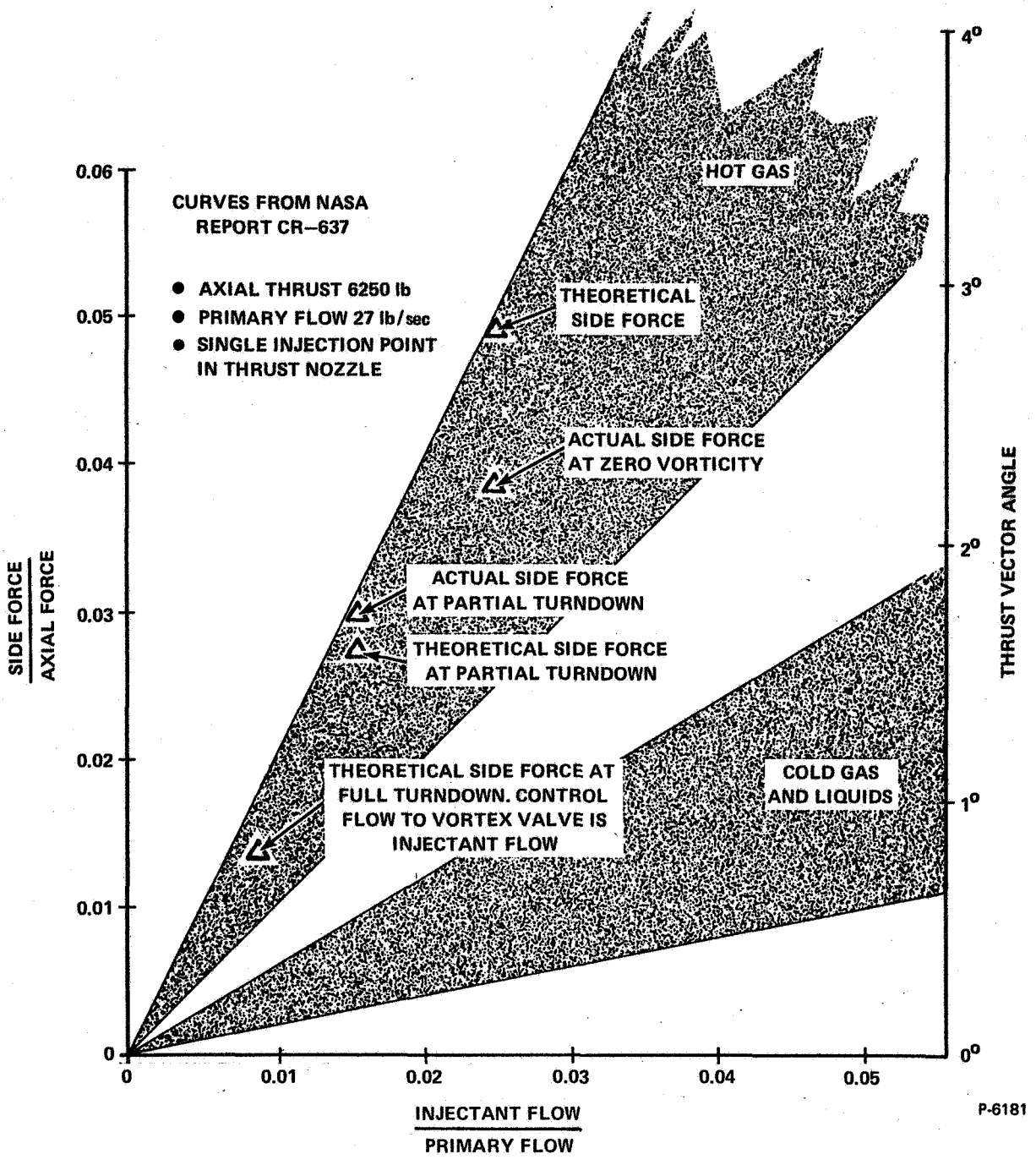

Figure 33 - Effectiveness of Hot Gas Injection Compared to Cold Gas and Liquid Injectants

flow into the thrust nozzle. A defection of the thrust vector would occur only when the injected flows result in a net differential flow.

The decrease in amplitude of ΔF yaw and ΔF pitch forces for increases in command signal frequency was attributed mainly to test stand response limitations. The dynamic sinusoidal frequency response of the SITVC system pilot stage control pressure, main stage control pressure, and EM-72 rocket motor yaw and pitch forces, as obtained from the hot gas test data, is shown in Figures 34 through 37. The main stage vortex valve outlet pressure was not plotted because of the failure of the "weeping orifice" flow measurement system. Also, shown in these figures is the theoretical dynamic frequency response of the pilot stage (P37 and P35) control pressure, main stage control pressure, and main stage outlet pressure (or secondary injectant supply pressure). Theoretical data provide a close correlation to the actual test data in most areas and indicate that there should be very little loss in amplitude or increase in phase lag across the main stage vortex valves. With these considerations, it can be assumed, as an approximation, that the frequency response of the vortex valve controlled SITVC system during the hot gas test was approximately the same as the hot gas main stage vortex valve control stage response. The data show that the control pressure P39 had an amplitude attenuation of -2.2 db and a phase lag of 68 degrees at 16 hertz while the rocket motor pitch forces recorded had an amplitude attenuation of -6.2 db and a phase lag of 122 degrees with the same command signal. These results indicate that the pitch SITVC command signal amplitude was attenuated -4 db and the phase lag increased 54 degrees between the main stage input command and the output pitch force. In the yaw plane the control pressure P41 signal amplitude was attenuated -8.5 db and the phase lag increased by 70 degrees between the input command and the output yaw force at a command signal frequency of 8 hertz.

Dynamic frequency response obtained for the SITVC system during the hot gas test is not representative of a final design configuration such as shown in Figure 1. The response of the SITVC system tested was compromised by the large control system manifold volumes that resulted from the inherent system design required for push-pull operation with one pilot stage controlling two SITVC vortex valves. A flyable vortex valve controlled system would achieve better response performance by using individual, close-coupled pilot stages for each SITVC vortex valve.

During the hot gas test, EM-72 rocket motor exhaust nozzle pressures were monitored and the resulting data plotted on a nozzle pressure map. Data shown in Figures 38(a) through 38(k) are typical data and cover one system cycle starting at 4.155 seconds. The shock patterns shown are estimated from the pressure distribution at the particular time and from the change in injectant flow.

The vortex valve controlled SITVC system structure and material contained the flow of aluminized 5500°F gas and 2000°F gas for the duration of the 50-second test without any structural failures. Components of the SITVC vortex valves are shown in Figure 39.

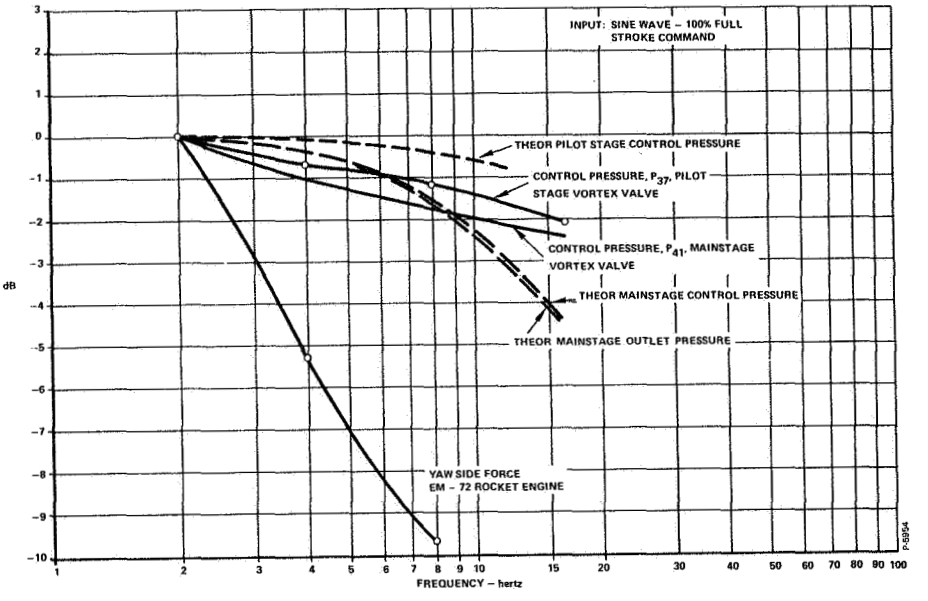

Figure 34 - Amplitude Versus Frequency, Yaw Plane of Vortex Valve Controlled SITVC System on EM-72 Rocket Engine

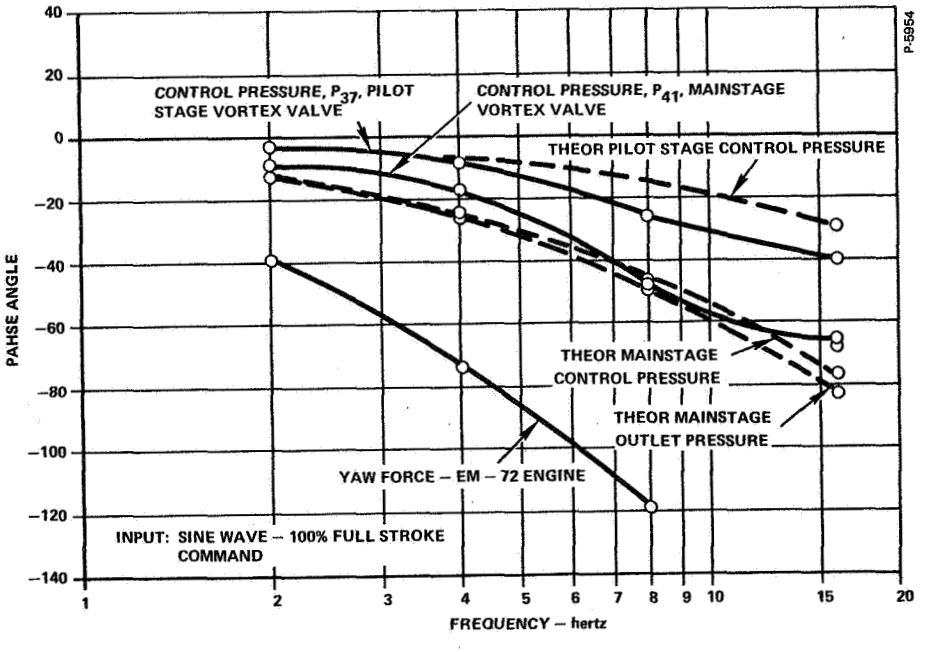

Figure 35 - Phase Angle Versus Frequency, Yaw Plane of Vortex Valve Controlled SITVC System on EM-72 Rocket Engine

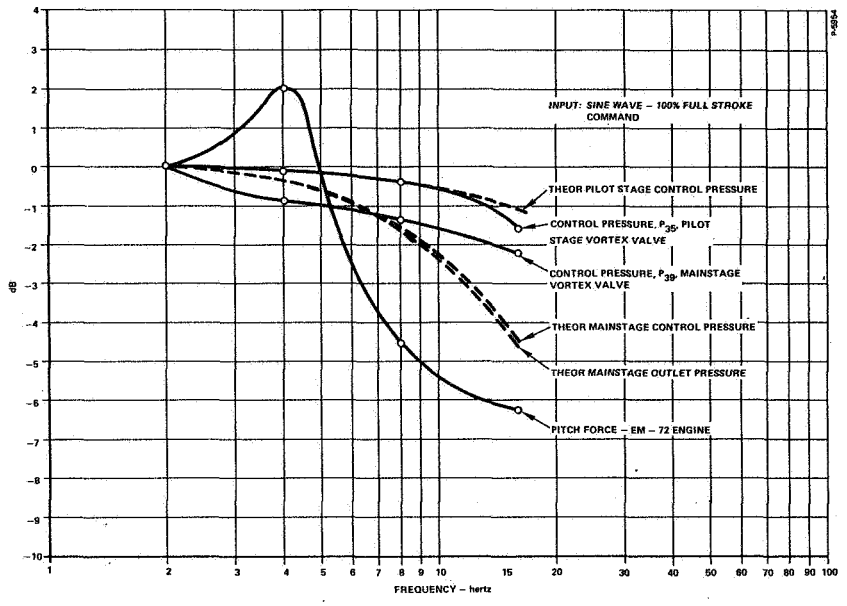

Figure 36 - Amplitude Versus Frequency, Pitch Plane of Vortex Controlled SITVC System on EM-72 Rocket Engine

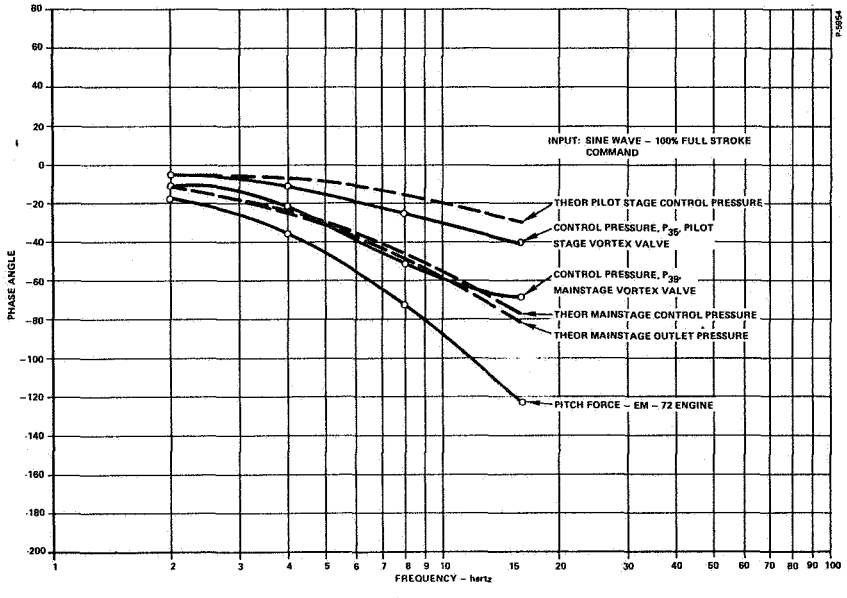

Figure 37 - Phase Angle Versus Frequency, Pitch Plane of Vortex Valve Controlled SITVC System on EM-72 Rocket Engine

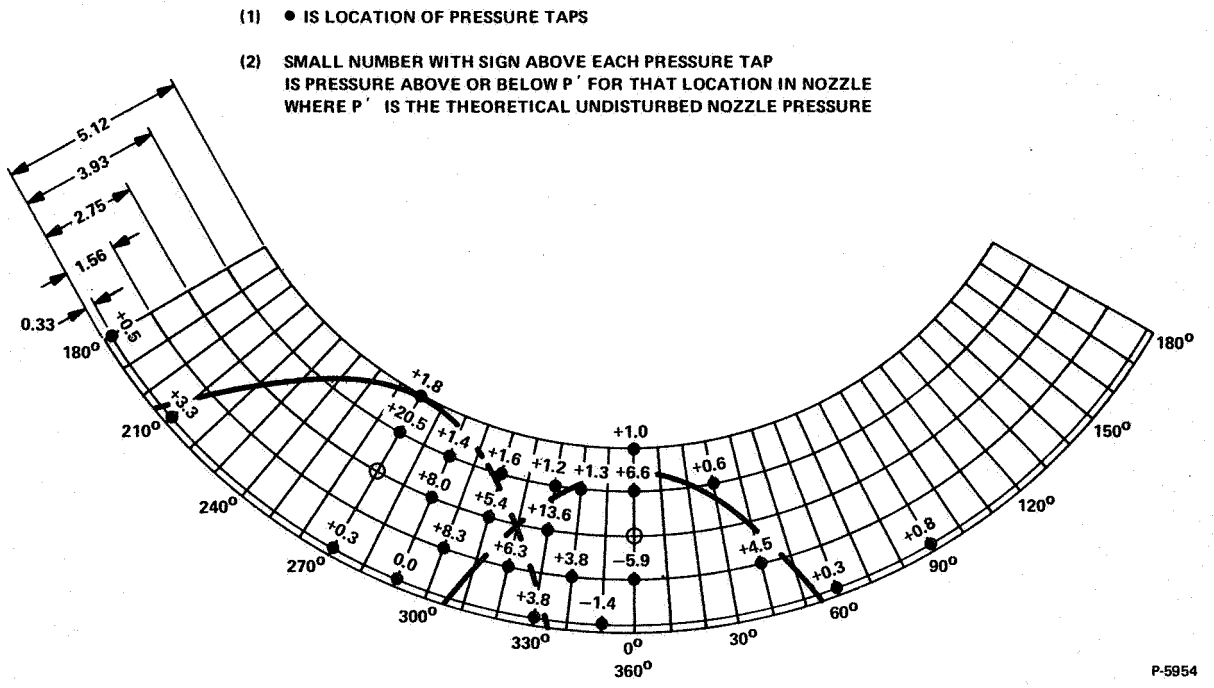

Figure 38(a) - Nozzle Pressure Probe Map - Time 4.155

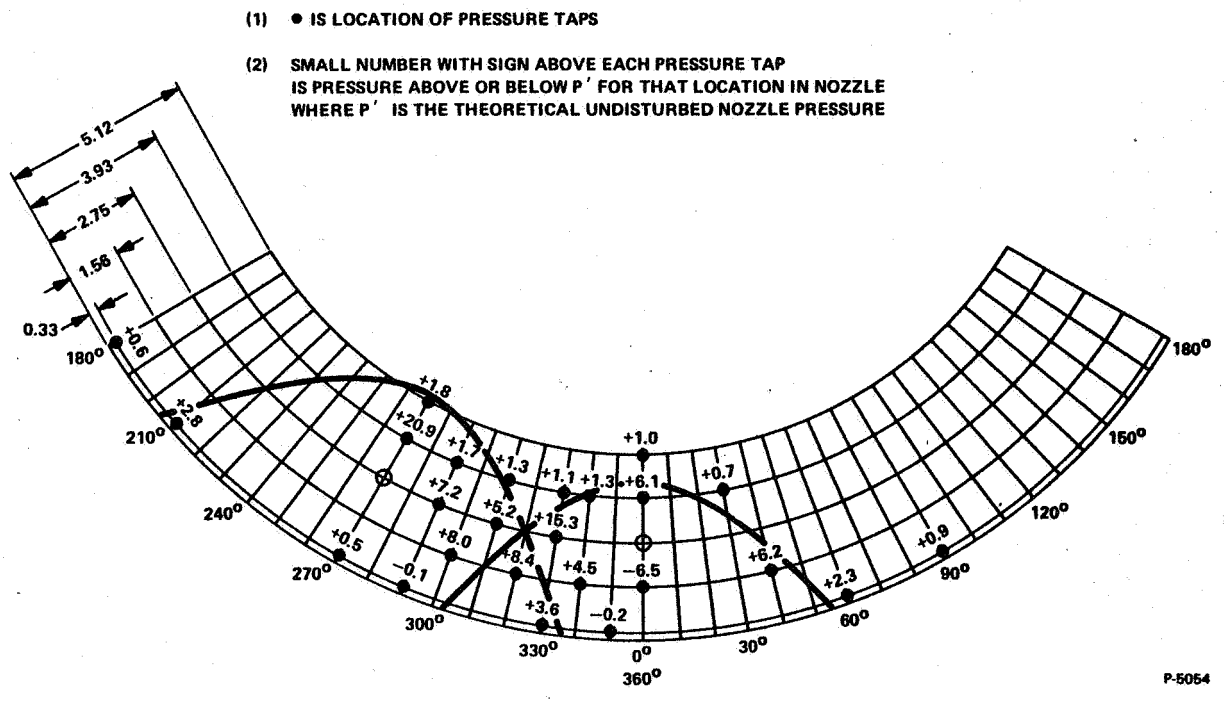

Figure 38(b) - Nozzle Pressure Probe Map - Time 4.187

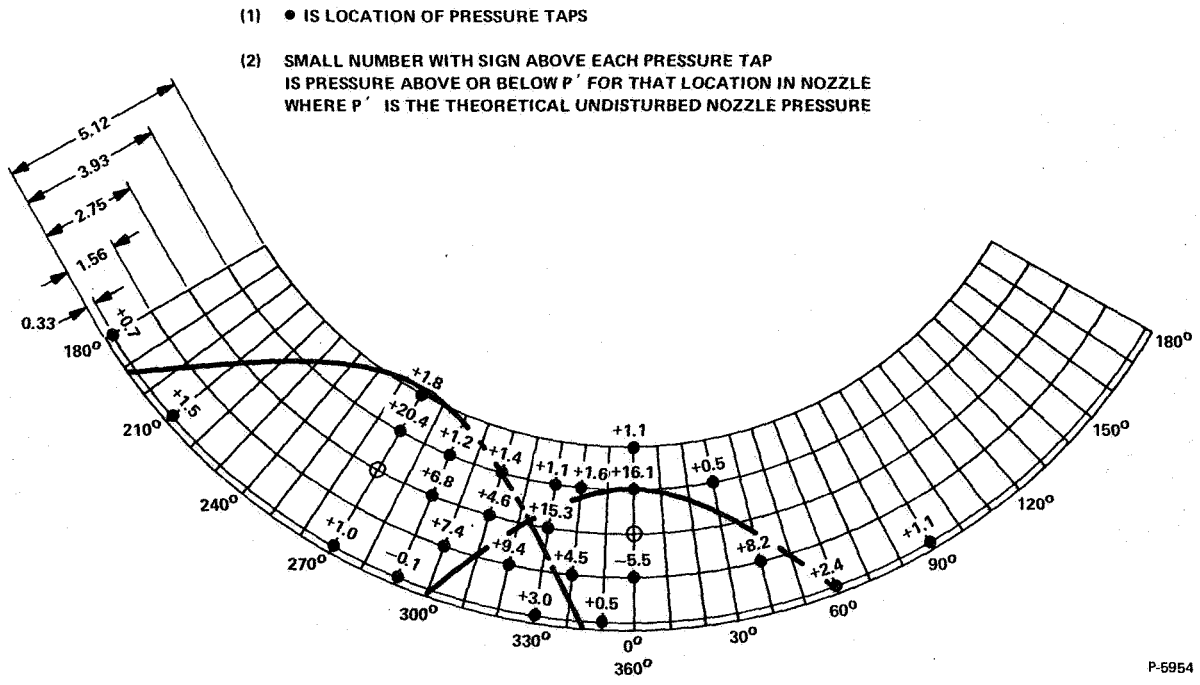

Figure 38(c) - Nozzle Pressure Probe Map - Time 4.220

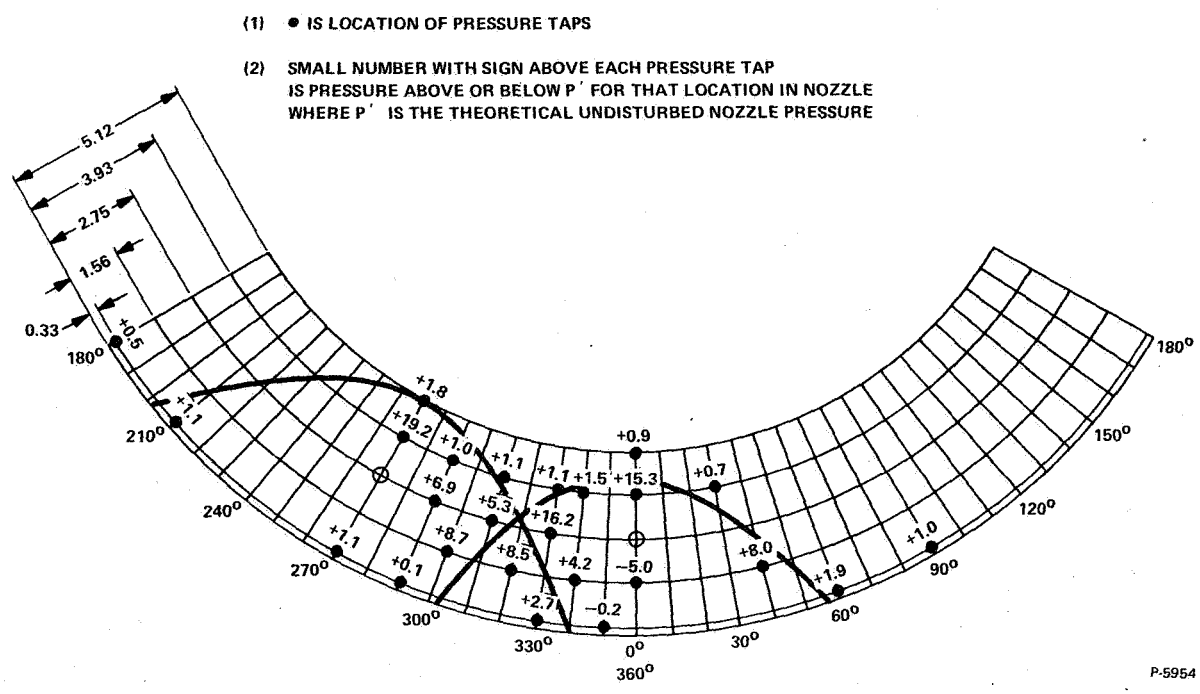

Figure 38(d) - Nozzle Pressure Probe Map - Time 4.255

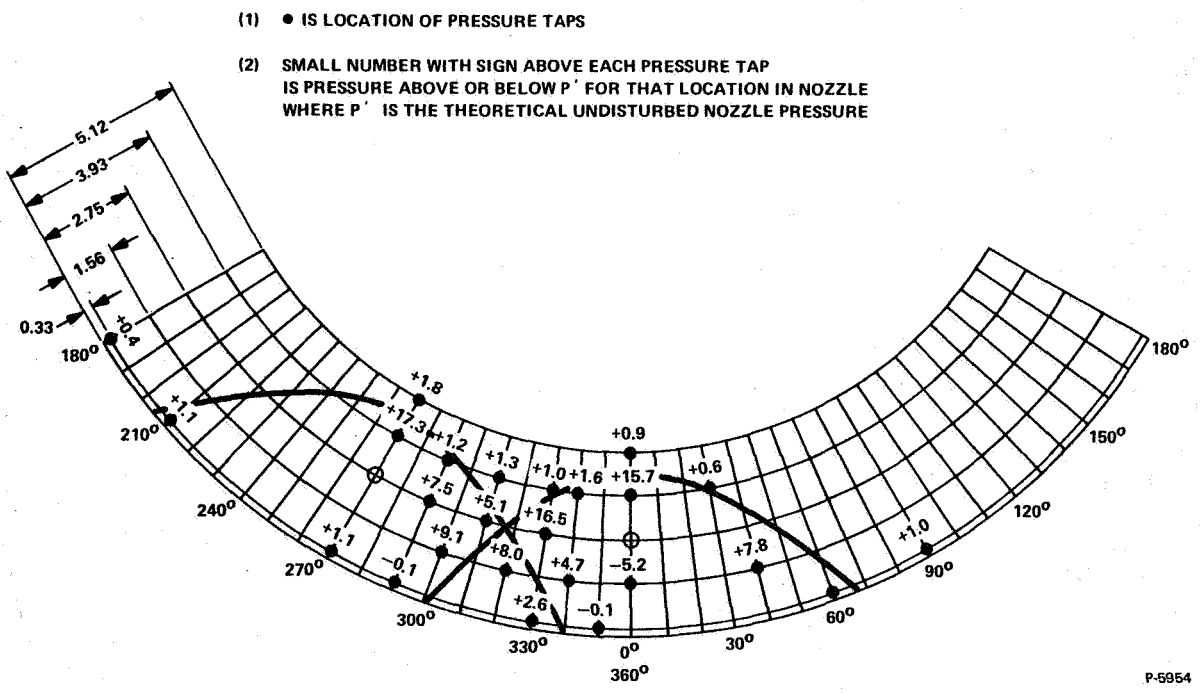

Figure 38(e) - Nozzle Pressure Probe Map - Time 4.285

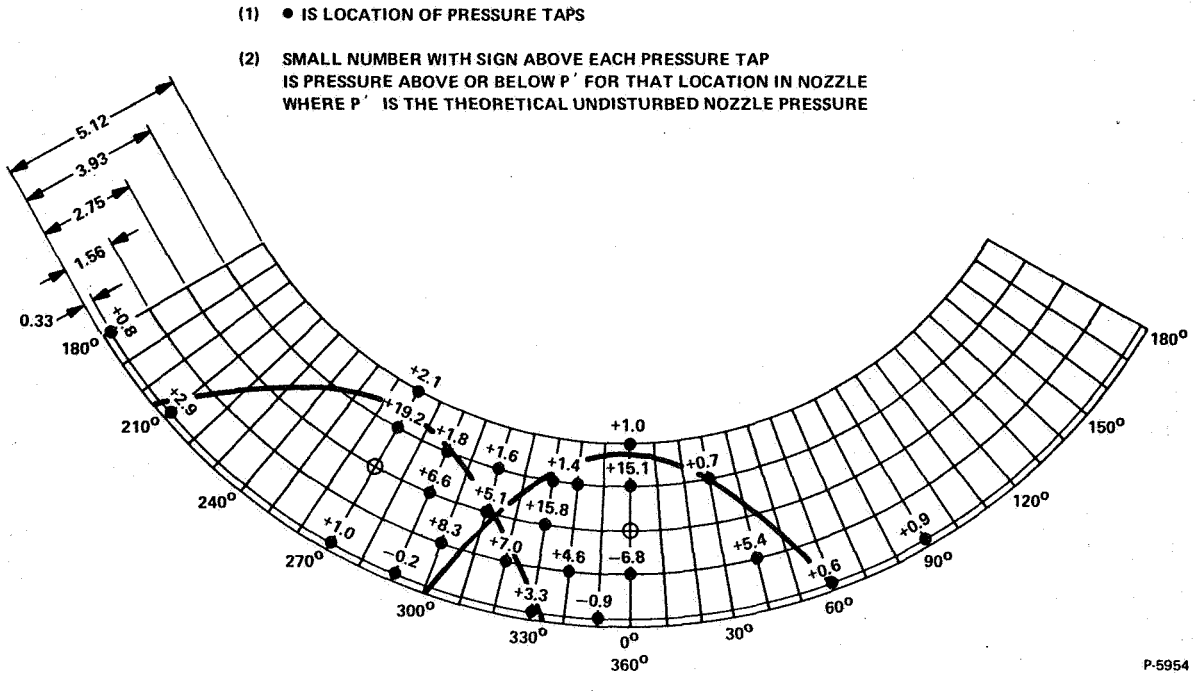

Figure 38(f) - Nozzle Pressure Probe Map - Time 4.318

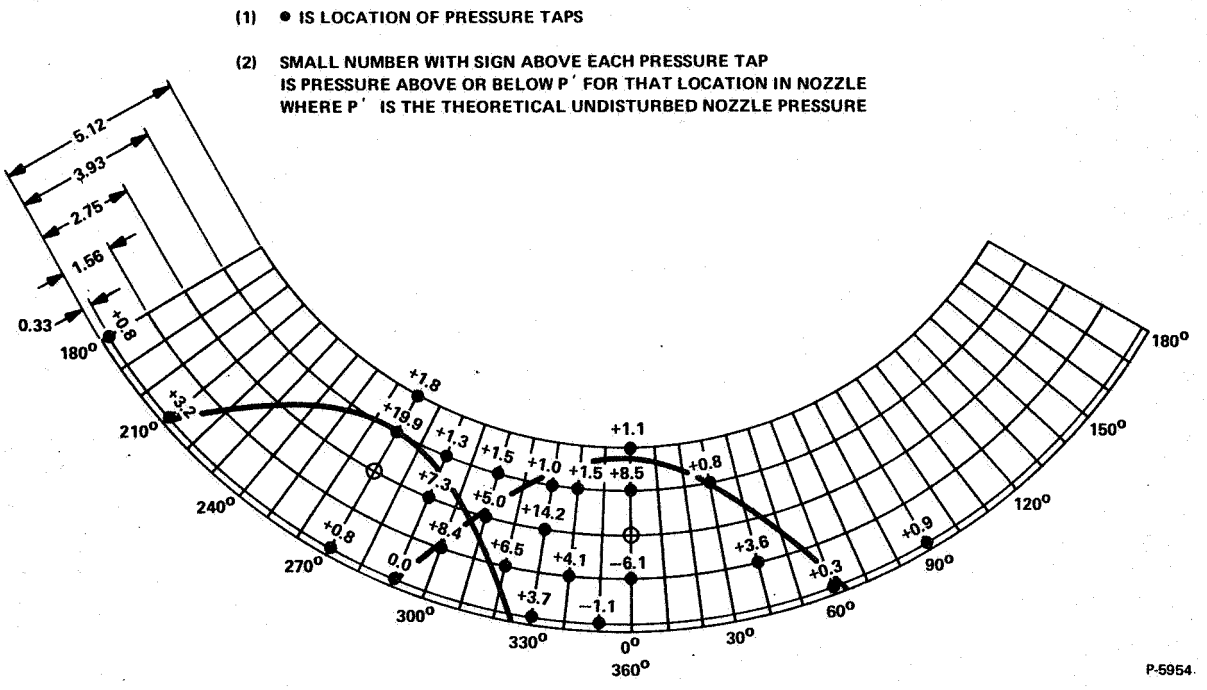

Figure 38(g) - Nozzle Pressure Probe Map - Time 4.351

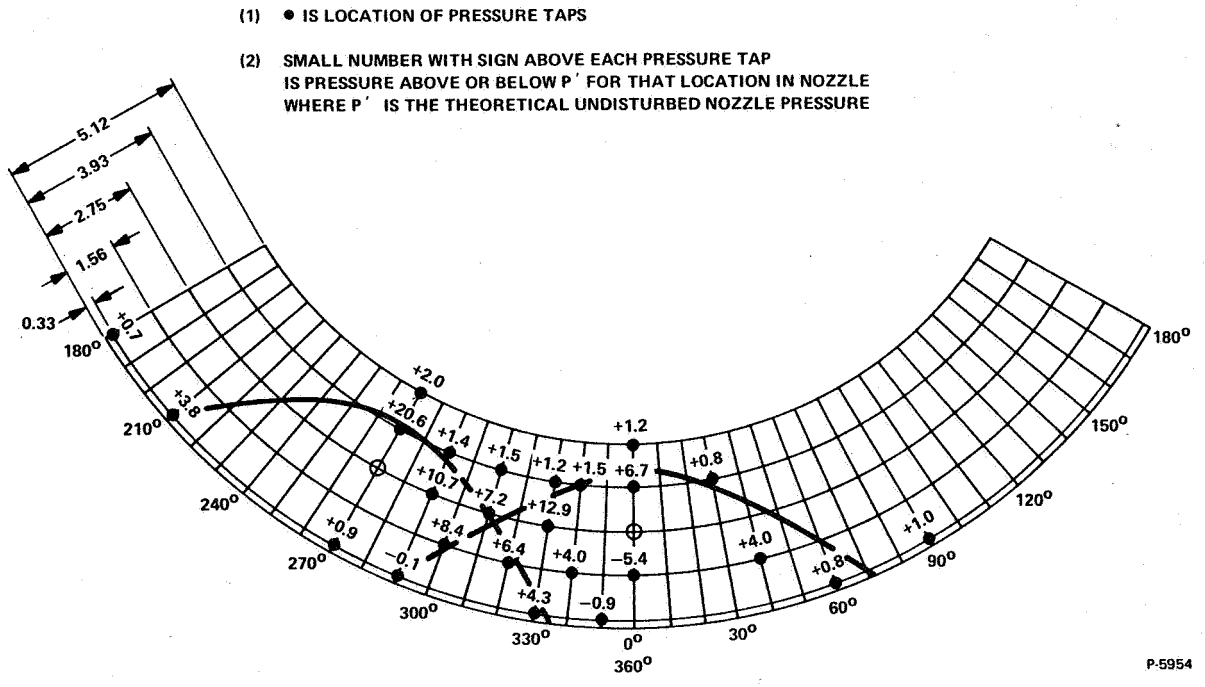

Figure 38(h) - Nozzle Pressure Probe Map - Time 4.387

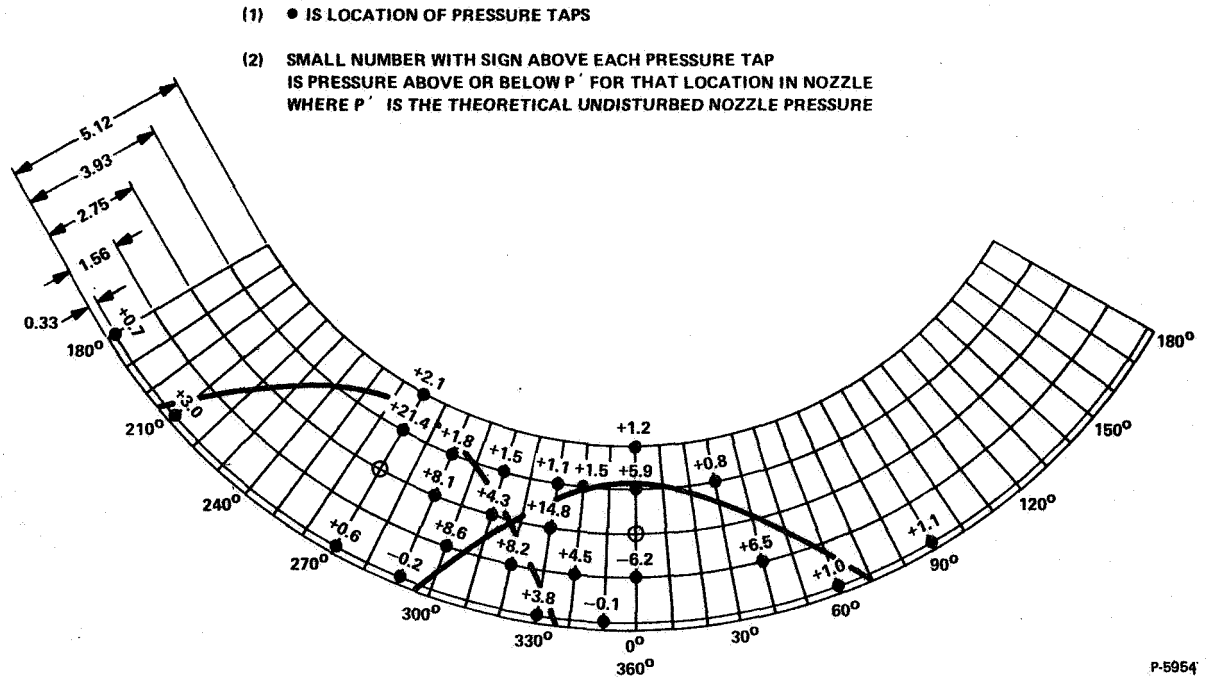

Figure 38(i) - Nozzle Pressure Probe Map - Time 4.420

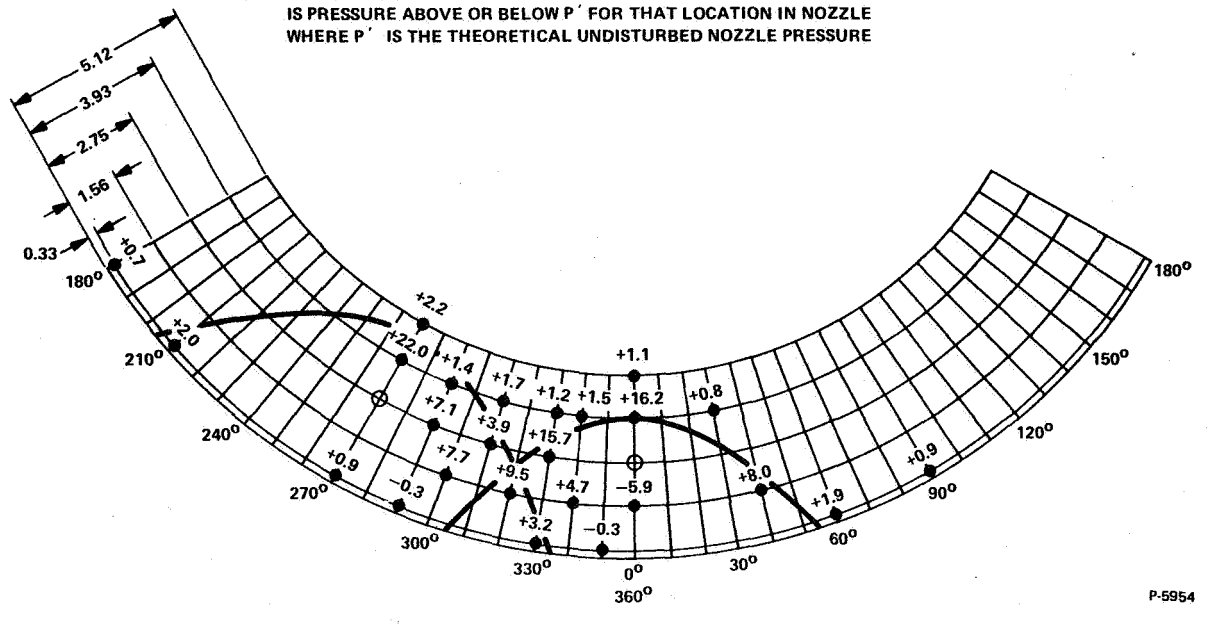

Figure 38(j) - Nozzle Pressure Probe Map - Time 4.452

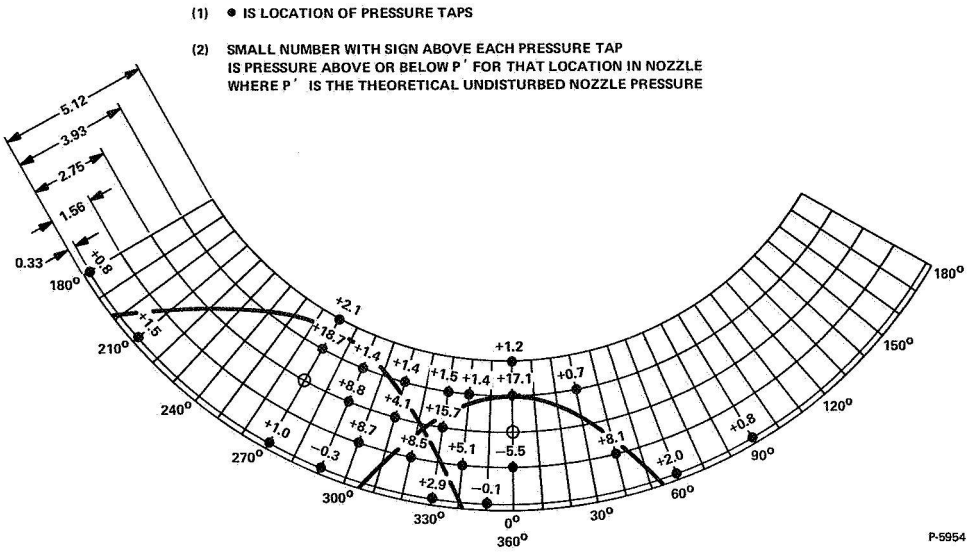

Figure 38(k) - Nozzle Pressure Probe Map - Time 4.485

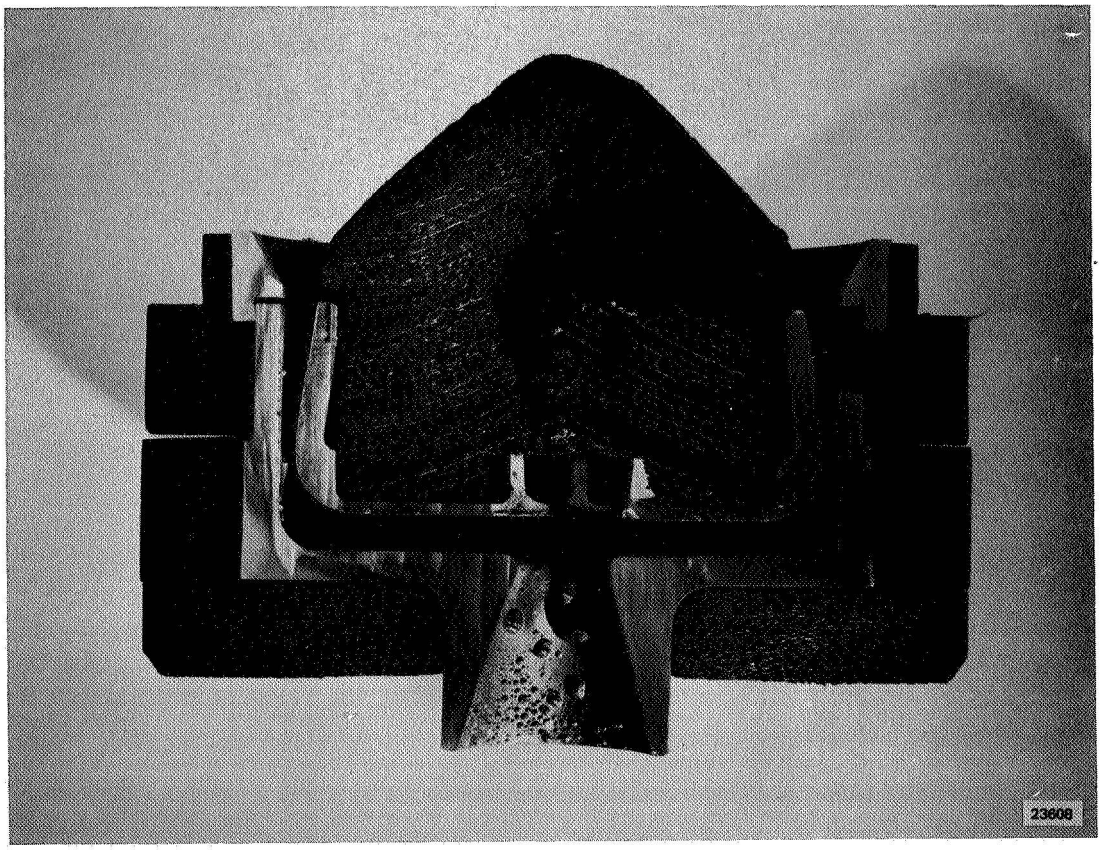

Figure 39 - Post Test, Interior of Hot Gas SITVC Vortex Valve

Test Conclusions

Examination of the test data and hardware led to the following hot gas test conclusions:

(1) Test pressure data showed that the vortex valve controlled SITVC system components were of the proper proportions to obtain desired system pressure distribution but that the auxiliary gas generators operated at pressures lower than expected.

(2) The SITVC vortex valves modulated the flow of aluminized 5500°F secondary injection gas that produced yaw and pitch forces on the rocket motor at frequencies of 2, 4, 8, and 16 hertz for 16 seconds of the test time.

(3) SITVC system frequency response to a sinusoidal control input showed an estimated amplitude ratio attenuation of -2.2 db and a phase lag of 68 degrees at 16 hertz. The large control manifold volumes, necessitated by the hardware packaging problem, were primarily responsible for the apparent low frequency response.

(4) The pilot stage torque motor began malfunctioning at 16 seconds, which was 4 seconds after rocket motor burnout, and thus affected the "engine out" portion of the test.

(5) The "weeping orifice" flow measurement system did not function due to plugging of the pressure measurement ports with aluminum oxide which solidified from the hot gas.

(6) The SITVC system handled the flow of alumininized 5500°F gas and 2000°F gas for over 50 seconds with no structural or material failures.

CONCLUSIONS AND RECOMMENDATIONS

Conclusions

This program demonstrated the application of the vortex valve, a no-moving-part fluidic device, as a valving element for controlling the flow of highly aluminized 5500°F solid propellant gas to obtain secondary injection thrust vector control of a solid propellant rocket motor. The following conclusions were drawn from the results of this program:

(1) The vortex valve utilized in this program is capable of handling 1 lb/sec flow of highly aluminized 5500°F solid propellant gas for more than 50 seconds. The vortex valve is a suitable valving element for throttling the flow of hot gas from high performance rocket motors in applications requiring direct chamber bleed gas control such as SITVC Systems or engine throttling applications.

(2) The vortex valve controlled SITVC System injectant pressure frequency response to sinusoidal control inputs showed an amplitude ratio attenuation of -2.2 db and a phase lag of 68 degrees at 16 hertz. This SITVC System design was based on mechanical simplicity. Through the use of integrated components, to reduce manifold volumes, dynamic system performance could be greatly improved.

(3) The ratio of side forces to injectant flow rate is within the band expected for hot gas injection. No large loss is apparent for a rotating injectant flow as generated by a vortex valve.

Recommendations

The experience gained from the demonstration of the hot gas vortex valve controlled SITVC System results in the following recommendations for the future.

(1) A vortex valve controlled SITVC System should be demonstrated on a rocket motor using direct chamber bleed gas from the rocket engine as the injectant. The recent design trend of buried nozzle rocket motors provides a practical configuration for such a demonstration. The high differential pressure available between the thrust chamber and the divergent nozzle section requires that a vortex valve be located in the thrust chamber with the outlet hole becoming the injection port. Four such valves can provide complete pitch and yaw thrust vector control on a rocket motor. Larger rocket motors may require multiple valves in each quadrant.

(2) It is recommended that a new pilot stage be designed to allow for the individual control of the main stage vortex valves rather than the push-pull type of operation of a pair of valves. A simple orifice and flapper-nozzle valve type of pilot stage would be more compatible with SITVC system installation and performance requirements for small rocket motors.

(3) The system tested to date has been a heavyweight, workhorse-type. Enough experience with materials has been acquired in this development program to permit the design of flightweight hardware. Concurrent with such design should be a weight tradeoff study to establish the competitive position of the vortex valve controlled secondary injection control system in comparison with other types of thrust vector control. It is recommended that all future efforts be accomplished with flightworthy hardware.

(4) It is recommended that additional effort be made toward the development of a technique for measuring the flow of aluminized 5500°F solid propellant gases. Since materials have been used in this program which survive for reasonable periods of time in this environment, it appears that the design and development of a reliable hot gas flow measurement device is possible.

(5) It is recommended that other applications of the hot gas vortex valve, such as for thrust control of a solid rocket motor, be investigated.

APPENDIX

SITVC PERFORMANCE ANALYSIS

The hot gas test performance of the vortex valve controlled SITVC System was evaluated by comparing observed test results with theoretical performance estimates. The evaluation was made for the yaw SITVC valve at test time 4.3 seconds. The pitch SITVC valve was not evaluated due to lack of data that would allow accurate separation of SITVC pitch forces from changes in EM-72 engine propellant weight losses and center-of-gravity shifts that occurred during the test.

Since the flow measurement system failed to function during the test, the secondary injection hot gas flows required to obtain theoretical yaw forces were calculated from available pressure data and orifice sizes.

Hot Gas Flow Calculations

The deduced maximum and minimum hot gas flows and the theoretically possible, fully turned down, minimum hot gas flow through the yaw SITVC vortex valve for system conditions at test time 4.3 seconds (Figure 23) aredetermined below.

By assuming that the yaw SITVC vortex valve is a simple sonic orifice when its P_c/P_s ratio is 1.08 to 1, the maximum yaw valve hot gas flow was determined to be:

$$\dot{W}_{yaw(test\ max.)} = \dot{W}_2 = \frac{C_d\ C_2\ A_2\ P_{43}}{\sqrt{T_{43}}} = \frac{0.84\ (0.556)\ 0.237\ (474)}{\sqrt{6000}}$$

$$\dot{W}_{yaw(test\ max.)} = 0.676\ \text{lb/sec.}$$

The theoretical minimum yaw valve flow possible with the flow of 6000°R gas completely turned off was found by assuming that the yaw valve control injectors, A_1, are sonic orifices and that these injectors are the only yaw valve gas source. The theoretical minimum yaw valve flow is:

$$\dot{W}_{yaw(theo.\ min.)} = \dot{W}_{1(max.)} = \frac{C_d\ C_2\ A_1\ P_{41}}{\sqrt{T_{41}}} = \frac{0.74\ (0.412)\ 0.04\ (869)}{\sqrt{2360}}$$

$$\dot{W}_{yaw(theo.\ min.)} = 0.218\ \text{lb/sec.}$$

The minimum yaw valve flow was obtained by assuming that the pitch vortex valve was flowing at maximum and that the yaw valve flow was equal to the 5500°F SPGG output ($\dot{W}_{43}$) minus the pitch valve flow ($\dot{W}_{5(min.)}$) plus the yaw valve maximum control flow ($\dot{W}_{1(max.)}$).

The 5500°F SPGG output is:

$$\dot{W}_{43} = A_g \rho C P^n = 48 \ (0.0637) \ 0.044 \ P^{0.3} = 0.869 \text{ lb/sec.}$$

The maximum pitch vortex valve flow is:

$$\dot{W}_{5(min.)} = \frac{C_d C_2 A_5 P_{43}}{\sqrt{T_{43}}} = \frac{0.84 \ (0.556) \ 0.237 \ (474)}{\sqrt{6000}} = 0.676 \text{ lb/sec.}$$

Therefore, the minimum yaw valve flow is:

$$\dot{W}_{yaw(test\ min.)} = \dot{W}_{43} - \dot{W}_{5(max.)} + \dot{W}_{1(max.)} = 0.869 - 0.676 + 0.218$$

$$\dot{W}_{yaw(test\ min.)} = 0.411 \text{ lb/sec.}$$

Side Force Calculations

Theoretical yaw plane side forces were calculated for the three yaw vortex valve flow conditions considered in the flow calculations above. The side force computations were made utilizing a procedure reported in Reference No. 2 and outlined below.

The first step in the side force computation was to locate the shock pattern in the primary nozzle that resulted from each of the three secondary injection flows. The shock patterns were located using the following trial-and-error procedure:

(1) Assume an M_o.

(2) Obtain D_o and P_o from Figure 42.

(3) Calculate L_s; $L_s = \frac{D_e - D_o}{2 \tan \alpha}$

(4) Obtain δ, θ, $\frac{\overline{P}_2}{P_o}$, and $\frac{P_s}{P_o}$ from Figure 41.

(5) Calculate $\overline{P}_s$; $\overline{P}_s = \frac{1}{3}(2 P_s + P_j)$.

(6) Calculate h; $h = \left\{ \frac{0.811 (A_j^* P_{jc} \Gamma)^2}{(\overline{P}_s - P_o)[(\gamma_j + 1) P_o + (\gamma_j - 1) \overline{P}_s]} \right\}^{1/4}$

where

$$\Gamma = \left(\frac{2}{\gamma + 1} \right)^{\frac{\gamma+1}{2(\gamma-1)}} \quad ; \text{ and for } \gamma_j = 1.3, \Gamma = 0.761$$

(7) Calculate X; $X = h [\cos \delta + \tan (\alpha + \varepsilon)]$.

(8) Test for L_s; $L_s = L_j + X \cos \alpha$.

(9) If L_s from step 8 does not match that of step 3, assume a new M, and repeat process.

The parameters and variables used in these computations are shown in Figures 40, 41, and 42, and Table 2.

By utilizing some of the above parameters and the estimated shock pattern information, the yaw side forces were found from the following equation:

$$F_s = \left[\left(\frac{\overline{P}_2}{P_o} - 1 \right) \left(X^2 \tan \theta - Xh \right) + \left(\frac{P_s}{P_o} - 1 \right) \left(Xh - \frac{A_j}{2} \right) \right] P_o \cos \alpha$$

$$+ \left[\left(P_j - P_o \right) A_j + \frac{\dot{w}_j v_j}{g} \right] \cos \varepsilon$$

This equation for side force determination contains the following four expressions which have the meanings indicated.

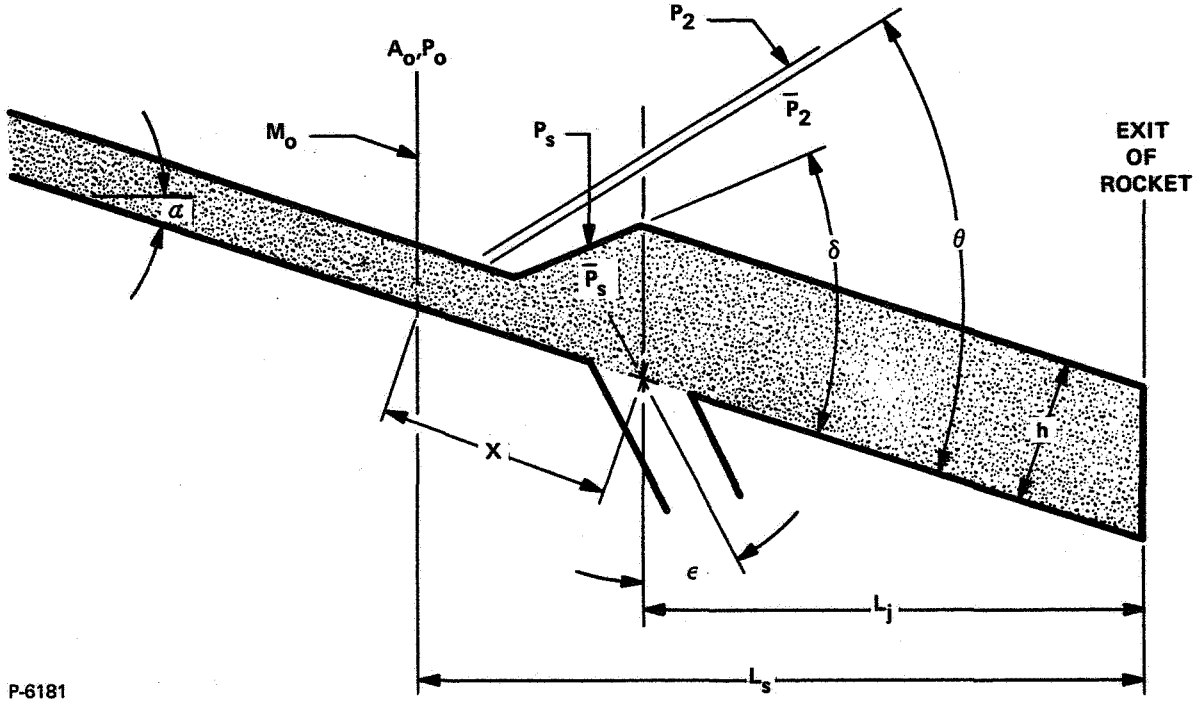

P_o	PRIMARY STREAM PRESSURE AT SHOCK APEX
P_2	PRESSURE ALONG SHOCK
$\bar{P}_2$	AVERAGE PRESSURE IN SHOCK REGION
P_s	PRESSURE ON THE SEPARATED BOUNDARY LAYER
$\bar{P}_s$	AVERAGE PRESSURE IN SEPARATED REGION
h	ACCOMMODATE HEIGHT
L_j	DISTANCE BETWEEN INJECTION POINT AND EXIT
L_s	DISTANCE BETWEEN SHOCK APEX AND EXIT
X	DISTANCE BETWEEN SHOCK APEX AND INJECTION POINT
ϵ	INJECTION ANGLE
α	NOZZLE HALF-ANGLE

Figure 40 - System Parameters and Variables

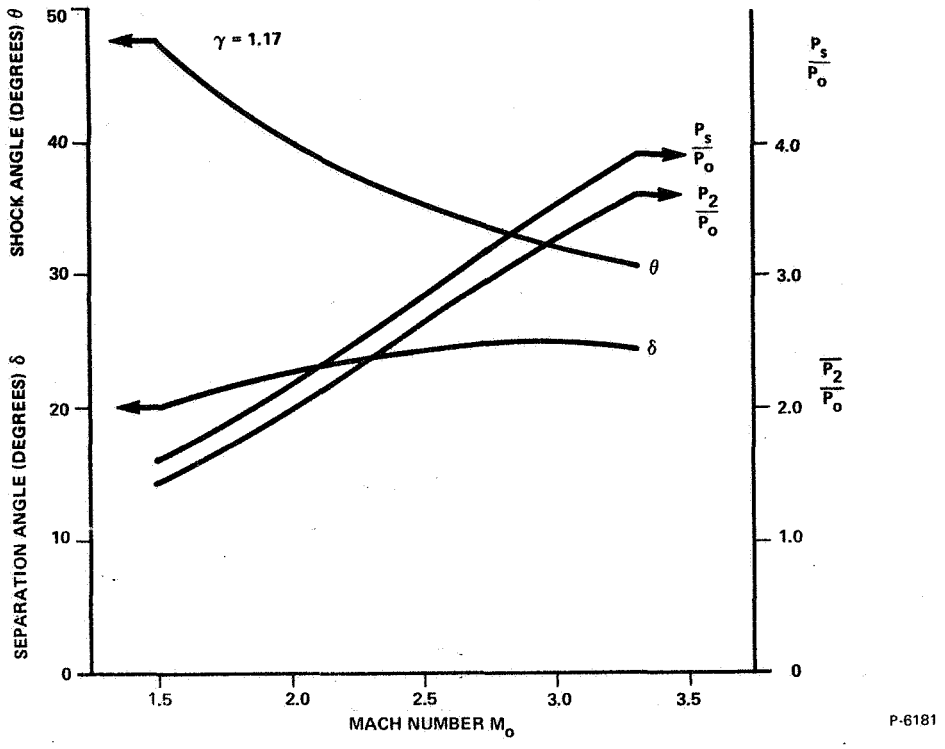

Figure 41 - Shock Angle, Separation Angle and Pressure Ratios Versus Primary Mach Number at Shock Apex

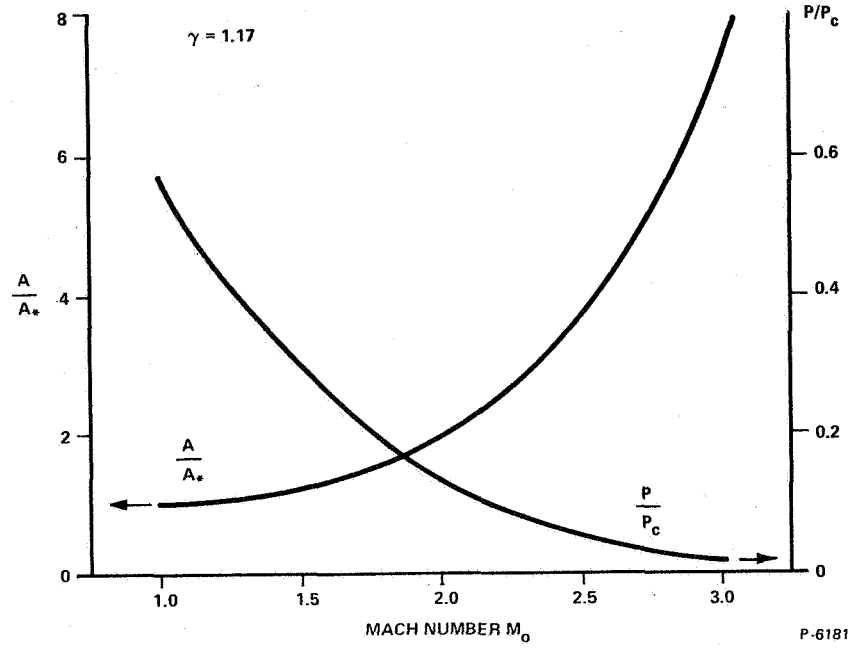

Figure 42 - Area Ratio, Pressure Ratio Versus Primary Mach Number

Table 2 - Side Force Calculation Parameters

Parameters / Side Force Conditions		Max. Yaw Test Flow	Min. Yaw Test Flow	Min. Yaw Theo. Flow
A_j^* (in^2)	Injection nozzle throat area	0.388	0.388	0.388
A_j (in^2)	A_j^* Injection nozzle exit area	0.388	0.388	0.388
D_j (in.)	Diameter of motor nozzle in plane of injection	7.65	7.65	7.65
D_e (in.)	Diameter of motor nozzle in exit plane	9.14	9.14	9.14
L_j (in.)	Distance from injection plane to nozzle exit plane parallel to nozzle axis	2.75	2.75	2.75
P_j	Injection nozzle exit pressure	158	93	42.5
P_{jc}	Injection nozzle chamber pressure	270	158	77.6
v_j	Injection nozzle exit velocity	3580	2920	2860
$\dot{W}_j$	Injection nozzle weight flow	0.676	0.411	0.218
α (deg.)	Primary nozzle half-angle	15°	15°	15°
γ (deg.)	Specific heat ratio primary gas	1.3	1.3	1.3
ε (deg.)	Angle between injection nozzle centerline and a line perpendicular to the motor nozzle axis	0°	0°	0°
T_j (°R)	Injectant gas temperature	6000	4000	2360

P-6181

(1) $\left[\left(\frac{\overline{P}_2}{P_o} - 1\right)\left(X^2 \tan\theta - Xh\right)\right] P_o \cos\alpha$ [pressure increase between shock and separated region]

(2) $\left[\left(\frac{P_s}{P_o} - 1\right)\left(Xh - \frac{A_j}{2}\right)\right] P_o \cos\alpha$ [pressure increase in separated region]

(3) $(P_j - P_o) A_j \cos\varepsilon$ [pressure difference $P_j - P_o$ acting on injection nozzle area]

(4) $\frac{\dot{w}_j v_j}{g} \cos\varepsilon$ [momentum effect of injected gas]

The results of yaw side force calculations for the three secondary injection flow conditions are shown in Table 3 and Figure 38(a).

Table 3 - Results of Yaw Side Force Calculations

Parameters		Max. Yaw Test Flow	Min. Yaw Test Flow	Min. Yaw Theo. Flow
h(in.)	Accommodation height	0.878	0.66	0.62
L_s(in.)	Distance between shock apex and exit	5.00	4.34	4.25
$\overline{P}^2$(psia)	Avg. pressure in shock region	74.7	61	67
$\overline{P}_s$(psia)	Avg. pressure in separation region	115.6	65	72
δ(deg.)	Separation angle	24.2°	24.6°	24°
θ(deg.)	Shock angle	35	35.5	34.5
F_s(lb)	Side force (calc.)	303	171	89
F_j(lb)	Side force (measured)	239	186	--

P-6181

GLOSSARY OF SYMBOLS

A = orifice area, in^2

A_g = solid propellant grain cross-sectional area, in^2

c = solid propellant burn characteristic constant

C_d = orifice flow discharge coefficient

C_2 = thermodynamic gas constant, $°R^{1/2}/sec$

D = nozzle diameter, in.

F = side force

f_1 = orifice flow function

k = specific heat ratio

m_o = Mach No. - primary nozzle flow

n = solid propellant burn characteristic pressure exponent

N_2 = nitrogen gas

P = pressure, psia

$\bar{P}$ = average pressure, psia

P_c = vortex valve control pressure, psia

P_g = gas generator pressure, psia

P_s = vortex valve supply pressure, psia

$(P_d/P_u)_{crit.}$ = pneumatic critical pressure ratio

r = solid propellant burn rate, in/sec

SITVC = secondary injection thrust vector control

SPGG = solid propellant gas generator

T = temperature, °F or °R

$\dot{W}$ = gas weight flow, lb/sec

ρ = solid propellant grain density, lb/in^3

REFERENCES

1. Keranen, T. W., and Blatter, A., "Research and Development of a Vortex Valve for Flow Modulation of a 16-Percent Aluminized 5500°F Propellant Gas," prepared under NASA Contract NAS-1-5199 for Langley Research Center by Bendix Research Laboratories, September 1967.

2. Sperry Rand Corp., "Proportional Solid Propellant Secondary Injection Thrust Vector Control Study," NASA CR-637,prepared under NASA Contract NAS 1-2962 for Langley Research Center, November 1966.

BIBLIOGRAPHY

1. Holt, W. D., and Rivard, J. G., "Research Study of the Vortex Valve for Medium Temperature Solid Propellants," NASA CR-424, prepared under NASA Contract NAS 1-4158 for Langley Research Center by Bendix Research Laboratories, April 1966.

2. Sutton, G. P., Rocket Propulsion Elements, John Wiley & Sons, Incorporated.

3. Rivard, J. G., "Secondary Injection Thrust Vector Control Using Fluidic Vortex Valves," presented at Western Electronic Show and Convention, San Francisco, California, August 1967.

ABSTRACT

The flow of hot (5500°F) gas from a solid propellant gas generator has been successfully throttled by a fluidic, no-moving-part, vortex valve. The vortex valve has been demonstrated by the application of hot gas secondary injection thrust vector control to a solid propellant rocket motor. The hot gas vortex valves were controlled by a pilot stage utilizing a flapper-nozzle and vortex amplifier valve arrangement which modulated the flow of a 2000°F pilot stage solid propellant gas generator. Materials found suitable for the 5500°F hot gas application consist of silver-infiltrated tungsten, silica phenolic, carbon phenolic, and graphite phenolic.

REPORT DISTRIBUTION LIST FOR
CONTRACT NO. NAS1-5199

NASA Langley Research Center (2)
Langley Station
Hampton, Virginia 23365
Attention: Research Reports Division
Mail Stop 122

NASA Langley Research Center (1)
Langley Station
Hampton, Virginia 23365
Attention: R. L. Zavasky
Mail Stop 117

NASA Langley Research Center (5)
Langley Station
Hampton, Virginia 23365
Attention: John M. Riebe
Mail Stop 217

NASA Langley Research Center (1)
Langley Station
Hampton, Virginia 23365
Attention: Robert L. Swain
Mail Stop 217

NASA Langley Research Center (2)
Langley Station
Hampton, Virginia 23365
Attention: David J. Carter, Jr.
Mail Stop 498

NASA Ames Research Center (1)
Moffett Field, California 94035
Attention: Library, Stop 202-3

NASA Flight Research Center (1)
P. O. Box 273
Edwards, California 93523
Attention: Library

Jet Propulsion Laboratory (1)
4800 Oak Grove Drive
Pasadena, California 91103
Attention: Library, Mail 111-113

Jet Propulsion Laboratory (1)
4800 Oak Grove Drive
Pasadena, California 91103
Attention: Winston Gin
Mail Stop 125-159

Jet Propulsion Laboratory (3)
4800 Oak Grove Drive
Pasadena, California 91103
Attention: Warren L. Dowler
Mail Stop 125-159

NASA Manned Spacecraft Center (1)
2101 Webster Seabrook Road
Houston, Texas 77058
Attention: Library, Code BM6

NASA Manned Spacecraft Center (1)
2101 Webster Seabrook Road
Houston, Texas 77058
Attention: Joseph G. Thibodaux, Jr.
Code EP

NASA Marshall Space Flight Center (1)
Huntsville, Alabama 35812
Attention: Library

NASA Marshall Space Flight Center (1)
Huntsville, Alabama 35812
Attention: John Q. Miller
R-P&VE-PPS

NASA Wallops Station (1)
Wallops Island, Virginia 23337
Attention: Library

NASA Electronics Research Center (1)
575 Technology Square
Cambridge, Massachusetts 02139
Attention: Library

NASA Lewis Research Center (1)
21000 Brookpark Road
Cleveland, Ohio 44135
Attention: Library, Mail Stop 60-3

NASA Lewis Research Center (1)
21000 Brookpark Road
Cleveland, Ohio 44135
Attention: Carl C. Ciepluch
Mail Stop 500-205

NASA Goddard Space Flight Center (1)
Greenbelt, Maryland 20771
Attention: Library

NASA John F. Kennedy Space Center (1)
Kennedy Space Center, Florida 32899
Attention: Library, Code IS-CAS-42B

National Aeronautics and (1)
Space Administration
Washington, D. C. 20546
Attention: Library, Code USS-10

National Aeronautics and (1)
Space Administration
Washington, D. C. 20546
Attention: William Cohen, Code RPM

National Aeronautics and (1)
Space Administration
Washington, D. C. 20546
Attention: Michael Gruber, Code MAL

National Aeronautics and (1)
Space Administration
Washington, D. C. 20546
Attention: Dr. Robert S. Levine,
Code RPL

National Aeronautics and (1)
Space Administration
Washington, D. C. 20546
Attention: Joseph E. McGolrick,
Code SV

National Aeronautics and (1)
Space Administration
Washington, D. C. 20546
Attention: Ward W. Wilcox, Code RPX

National Aeronautics and (1)
Space Administration
Washington, D. C. 20546
Attention: David L. Winterhalter,
Code MAT

National Aeronautics and (1)
Space Administration
Washington, D. C. 20546
Attention: Richard J. Wisniewski,
Code RMD

National Aeronautics and (1)
Space Administration
Washington, D. C. 20546
Attention: Robert W. Ziem, Code RPS

Air Force Office of Scientific Research (1)
1400 Wilson Boulevard
Arlington, Virginia 22209
Attention: Code SREP

Air Force Rocket Propulsion Laboratory (1)
Edwards, California 93523
Attention: Code RPM

Air Force Rocket Propulsion Laboratory (1)
Edwards, California 93523
Attention: J. T. Edwards, Code RPMC

Air Force Systems Command (1)
Andrews Air Force Base
Washington, D. C. 20331
Attention: Code SCTR

U. S. Army Missile Command
Redstone Scientific Information Center (1)
Redstone Arsenal, Alabama 35809
Attention: Document Section

Army Research Office (1)
Box CM, Duke Station
Durham, North Carolina 27706
Attention: Code CRD-AA-IP

Ballistic Research Laboratories (1)
Aberdeen Proving Ground, Maryland 21005
Attention: Code AMXBR-1

Defense Documentation Center (1)
Cameron Station, Building 5
Alexandria, Virginia 22314
Attention: Code OSR-1

John Hopkins University (1)
Applied Physics Laboratory
8621 Georgia Avenue
Silver Spring, Maryland 20910
Attention: Chemical Propulsion
Information Agency

John Hopkins University (1)
Applied Physics Laboratory
8621 Georgia Avenue
Silver Spring, Maryland 20910
Attention: T. M. Gilliland

John Hopkins University (1)
Applied Physics Laboratory
8621 Georgia Avenue
Silver Spring, Maryland 20910
Attention: T. L. Reedy

Frankford Arsenal
Propellant & Eplo. Section
Philadelphia, Pennysylvania 19137
Attention: Library, C2500-B51-2

Naval Air Systems Command (1)
Main Navy Building
19th & Constitution Avenue, N.W.
Washington, D. C. 20360
Attention: Code AIR-330

Naval Air Systems Command (1)
Main Navy Building
19th & Constitution Avenue, N.W.
Washington, D. C. 20360
Attention: Code AIR-604

Naval Air Systems Command (1)
Main Navy Building
19th & Constitution Avenue, N.W.
Washington, D. C. 20360
Attention: Code AIR-5366

Naval Air Systems Command (1)
Main Navy Building
19th & Constitution Avenue, N.W.
Washington, D. C. 20360
Attention: Code AIR-5367

Naval Mission Center (1)
Point Mugu, California 93041
Attention: Technical Library,
Code 5632.2

Naval Ordnance Laboratory (1)
White Oak
Silver Spring, Maryland 20910
Attention: Library

Naval Ordnance System Command (1)
Washington, D. C. 20360
Attention: Code ORD-0331

Naval Ordnance System Command (1)
Washington, D. C. 20360
Attention: Code ORD-9132

Naval Ordnance Station (1)
Indian Head, Maryland 20640
Attention: Technical Library, Code EDL

Naval Postgraduate School (1)
Monterey, California 93940
Attention: Technical Reports Library,
Section 2124

Naval Research Laboratory (1)
4555 Overlook Avenue, S.W.
Washington, D. C. 20390
Attention: Code 2027

Naval Air Systems Command (1)
Main Navy Building
19th and Constitution Avenue, N.W.
Washington, D. C. 2-360
Attention: J. C. Ardinger

TRW Inc. (1)
One Space Park
Redondo Beach, California 90278
Attention: J. K. Beatty
Bldg. M-1, Room 1521

TRW Inc. (1)
One Space Park
Redondo Beach, California 90278
Attention: R. M. Moy,
Bldg. 01, Room 1081

TRW Inc. (1)
One Space Park
Redondo Beach, California 90278
Attention: D. F. Reeves,
Bldg. 01, Room 1160C

Naval Weapons Center (1)
China Lake, California 93557
Attention: Technical Library,
Code 753

Naval Weapons Center (1)
China Lake, California 93557
Attention: Dr. C. J. Thelen

Naval Weapons Center (1)
China Lake, California 93557
Attention: D. E. Ruff

Picatinny Arsenal (1)
Scientific and Technical
Information Branch
Dover, New Jersey 07801
Attention: Library, SMUPA-VA6

White Sands Missile Range (1)
White Sands Missile Range,
New Mexico 77058
Attention: Technical Library

Naval Ordnance Systems Command (1)
3617 Munitions Building
18th and Constitution Avenue, N.W.
Washington, D. C. 20037
Attention: R. F. Cassel

United Technology Corporation (1)
Sunnyvale, California 94088
Attention: A. G. Cattaneo,
Post Office 358

United Technology Corporation (1)
Sunnyvale, California 94088
Attention: G. S. Morefield,
Post Office 358

Aerojet-General Corporation (1)
Post Office Box 15847
Sacramento, California 95809
Attention: D. R. Collis

Aerojet-General Corporation (1)
Post Office Box 15847
Sacramento, California 95809
Attention: Dr. B. A. Simmons

Rocketdyne (1)
Solid Rocket Division
Post Office Box 548
McGregor, Texas 76657
Attention: J. M. Cunningham

Aerotherm Corporation (1)
460 California Avenue
Palo Alto, California 94306
Attention: T. J. Dahm

Hercules, Inc. (1)
Allegany Ballistics Laboratory
Post Office Box 210
Cumberland, Maryland 21502
Attention: D. G. Drewry

Hercules, Inc. (1)
Allegany Ballistics Laboratory
Post Office Box 210
Cumberland, Maryland 21502
Attention: D. J. Sine

Army Missile Command (1)
Redstone Arsenal, Alabama 35809
Attention: R. H. Fink

Army Missile Command (1)
Redstone Arsenal, Alabama 35809
Attention: B. D. Richardson

Army Material Command (1)
2705 T-7, Gravely Point
Washington, D. C. 20315
Attention: J. Gensior

Air Force Rocket Propulsion Laboratory (1)
Edwards, California 93523
Attention: Major J. R. Giancola, Code RPMN

Aerospace Corporation (1)
2400 East El Segundo Boulevard
El Segundo, California 90045
Attention: Dr. R. B. Gilbert

Aerospace Corporation (1)
2400 East El Segundo Boulevard
El Segundo, California 90045
Attention: C. Speisman

Bendix Corporation (1)
Research Laboratories Division
Southfield, Michigan 48076
Attention: T. W. Keranen

Lockheed Missiles and Space Company (1)
Post Office Box 504
Sunnyvale, California 94088
Attention: R. L. LeCount,
Dept. 65-12,
Bldg. 102

Lockheed Missiles and Space Company (1)
Post Office Box 504
Sunnyvale, California 94088
Attention: R. E. Matzdorff,
Dept. 55-11,
Bldg. 102

Lockheed Propulsion Company (1)
Post Office Box 111
Redlands, California 92374
Attention: Dr. A. M. Messner,
Dept. 2330, Bldg. 118

Naval Ordnance Systems Command (1)
3612 Munitions Building
18th and Constitution Avenue, N.W.
Washington, D. C. 20037
Attention: J. W. Murrin

Rocket Power, Inc. (1)
2275 East Foothill Boulevard
Pasadena, California 91107
Attention: Vice President

NASA Scientific and Technical
Information Facility (9 plus reproducible)
P.O. Box 33
College Park, Maryland 20740